



Inter-comparison of four models for smoothing satellite sensor time-series data to estimate vegetation phenology

Peter M. Atkinson^a, C. Jeganathan^{b,*}, Jadu Dash^a, Clement Atzberger^c

^a Global Environmental Change and Earth Observation Research Group, Geography and Environment, University of Southampton, Southampton SO17 1BJ, United Kingdom

^b Department of Remote Sensing, Birla Institute of Technology (BIT), Mesra, Ranchi-835215, Jharkhand, India

^c Institute for Surveying, Remote Sensing and Land Information, University of Natural Resources and Life Sciences (BOKU), Vienna, Austria

ARTICLE INFO

Article history:

Received 2 June 2011

Received in revised form 28 March 2012

Accepted 1 April 2012

Available online 5 May 2012

Keywords:

Phenology

MTCI

MERIS

Fourier

Double logistic

Asymmetric Gaussian

Whittaker smoother

Filter techniques

ABSTRACT

Several models have been fitted in the past to smooth time-series vegetation index data from different satellite sensors to estimate vegetation phenological parameters. However, differences between the models and fine tuning of model parameters lead to potential differences, uncertainty and bias between the results amongst users. The current research assessed four techniques: Fourier analysis, asymmetric Gaussian model, double logistic model and the Whittaker filter for smoothing multi-temporal satellite sensor observations with the ultimate purpose of deriving an appropriate annual vegetation growth cycle and estimating phenological parameters reliably. The research used Level 3 Medium Resolution Imaging Spectrometer (MERIS, spatial resolution ~4.6 km) Terrestrial Chlorophyll Index (MTCI) data over the years 2004 to 2006 composited at eight day intervals covering the Indian sub-continent. First, the four models were fitted to representative sample time-series of the major vegetation types in India, and the quality of the fit was analysed. Second, the effect of noise on model fitting was analysed by adding Gaussian noise to a standard profile. Finally, the four models were fitted to the whole study area to characterise variation in the quality of model fitting as a function of single and double vegetation seasons. These smoothed data were used to estimate the onset of greenness (OG), a major phenological parameter. The models were evaluated using the root mean square error (RMSE), Akaike Information Criteria (AIC), and Bayesian Information Criteria (BIC). The first test (fitting to representative sample time series) revealed the consistently superior performance of the Whittaker and Fourier approaches in most cases. The second test (fitting after the addition of Gaussian noise) revealed the superior performance of the double logistic and Fourier approaches. Finally, when the approaches were applied to the whole study, thus, including vegetation with different phenological profiles and multiple growing seasons (third test), it was found that it was necessary to tune each of the models according to the number of annual growing seasons to produce reliable fits. The double logistic and asymmetric Gaussian models did not perform well for areas with more than one growing season per year. The mean absolute deviation in OG derived from these models was a maximum (3 to 4 weeks) within the dry deciduous vegetation type and minimum (1 week) in evergreen vegetation. All techniques yielded consistent results over the south-western and north-eastern regions of India characterised by tropical climate.

© 2012 Elsevier Inc. All rights reserved.

1. Introduction

Changes in the timing of the seasonal cycle of terrestrial vegetation have been linked to inter-annual and multi-annual climatic change (Cleland et al., 2007). The last three decades of satellite sensor observations suggest that spring has advanced globally at a rate of 2 to 5 days per decade (Parmesan & Yohe, 2003; Root et al., 2003) and that senescence has been delayed by 0.3 to 1.6 days per decade (Menzel, 2002) mostly attributable to recent increases in global temperature (Parmesan, 2007). However, the phenological cycle, as well as the

effect of climate change on vegetation phenology, is species- and location-dependent. This means that global averages have limited value locally, and it is important to describe space-time changes in phenology. It is difficult to provide such a global scale picture using only ground observations of phenological events as only a few countries possess a sufficiently dense observation network (e.g. Germany). In contrast, satellite-based remote sensing data can be used to map vegetation phenological events at medium to coarse spatial resolution through repeat measurement over the entire globe (Jeong et al., 2011; Malingreau, 1986).

Due to ease of calculation, and its long history of use in the literature, most studies utilised the normalised difference vegetation index (NDVI) to estimate vegetative phenological parameters from space (Jeong et al., 2011; Myneni et al., 1997; Reed et al., 1994; White et al.,

* Corresponding author. Tel.: +91 651 2275444x631.

E-mail address: jegan_iirs@yahoo.com (C. Jeganathan).

2005). The NDVI has been calculated for this purpose from the Advanced Very High Resolution Radiometer (AVHRR), Moderate Resolution Imaging Spectro-radiometer (MODIS) (Beck et al., 2006; Yu et al., 2005), Système Pour L'Observation de la Terre (SPOT)-VEGETATION (VGT) (Atzberger & Eilers, 2011a) and Indian Remote Sensing (IRS)-Wide Field Sensor (WiFS) sensors (Joshi et al., 2006; Prasad et al., 2007). However, a general problem with satellite sensor observations is that the data may be affected by the atmosphere (e.g. alteration of reflectance values due to undetected sub-pixel clouds, atmospheric dust and aerosols, gaseous absorbers). In addition, bidirectional reflectance distribution function (BRDF) effects mean that the recorded signal may be sensitive to view and illumination angles. Due to the mixed signatures observed at medium to coarse spatial resolution it is also necessary to consider landscape (patchiness) dependent effects. Obviously, satellite sensors do not record specific phenological events (e.g. flowering), providing only a general measure of vegetation activity and growth. Fewer studies relied on the enhanced vegetation index (EVI) from the MODIS sensor (Zhang et al., 2003).

Several techniques were applied to reduce the systematic and non-systematic errors associated with the NDVI (Pinzon, 2002; Pinzon et al., 2004; Tucker et al., 2005). However, other limitations of the NDVI remain, such as saturation at high levels of vegetation biomass and chlorophyll concentration (Gitelson & Kaufman, 1998; Huete et al., 2002; Mutanga & Skidmore, 2004). Recently, Dash and Curran (2004) utilised the MEdium Resolution Imaging Spectrometer (MERIS), a sensor with high radiometric accuracy (Curran & Steele, 2005), to estimate an alternative vegetation index which is linearly related to canopy chlorophyll content. This index is referred to as the MERIS Terrestrial Chlorophyll Index (MTCI) (Dash & Curran, 2004). Dash et al. (2008) observed that the signal-to-noise ratio of temporal vegetation profiles from MTCI was significantly greater than the SNR of equivalent NDVI curves. Dash et al. (2010) and Jeganathan et al. (2010a,b) utilised time-series MTCI data to estimate phenological parameters for the tropical vegetation of India.

In most phenology studies using satellite sensor data the inevitable first step is to convert noisy temporal input vegetation index data into a smooth time-series, to estimate phenological parameters such as the onset of greenness (OG), length of season and end of senescence (ES). Several techniques have been used to correct and smooth such time-series vegetation index data, and to support the estimation of phenological parameters. Widely used methods in smoothing time-series satellite sensor data are: median smoothing (Reed et al., 1994), curve fitting (Bradley et al., 2007), moving average (White et al., 2009), Fourier decomposition (Jakubauskas et al., 2001; Moody & Johnson, 2001; Roerink et al., 2000; Verhoef et al., 1996; Wagenseil & Samimi, 2006), logistic function (Beck et al., 2006; Zhang et al., 2003), asymmetric Gaussian function (Jönsson & Eklundh, 2002), Savitzky–Golay filter (Chen et al., 2004), high order spline with roughness damping (Hernance et al., 2007) and wavelet decomposition (Lu et al., 2007; Sakamoto et al., 2005). Recently, the Whittaker smoother (Eilers, 2003) has also been adopted for smoothing remotely sensed time-series (Atzberger & Eilers, 2011a,b).

Each method has its own advantages and disadvantages, and the choice of model depends upon the purpose of the study (Hird & McDermid, 2009). Most models require fine tuning of parameters such as the noise-threshold, size of temporal neighbourhood and number of harmonics (Atkinson et al., 2009). Recently, de Beurs and Henebry (2010) surveyed 12 existing spatio-temporal statistical methods being used to estimate phenological parameters from time-series of satellite sensor data and revealed a lack of general consensus regarding nomenclature, model significance, uncertainty and error structure. Their research also revealed that it would be difficult to find a single set of parameters suitable for all the vegetation types of a diverse landscape. Hence, users are left to choose the parameter values, which may lead to differences in the derived information and lack of consistency between users.

Most of the models surveyed by de Beurs and Henebry (2010) were evaluated by fitting models to NDVI time-series for higher latitudinal regions. These models were fitted to the upper envelope of the data series (i.e., the fit was to values larger than the local mean) to adjust for the atmospherically-induced negative bias in NDVI (Holben, 1986). Unlike NDVI, MTCI is less affected by noise from the atmosphere and soil background, and there is no overall bias. Therefore, in MTCI data the noise can be assumed to be white (zero mean). Consequently, models should be fitted to the local mean, not the upper envelope.

The Forest Survey of India (FSI) has a satellite-based regular mapping and monitoring programme and publishes a national forest area assessment report on a two-yearly basis. However, official maps of phenology for India are still not available. The complexity in fitting algorithms, parameters and model choice, and data noise are likely hurdles to progress. Hence, it is interesting to evaluate models for smoothing time-series vegetation index (VI) data over the complex and diverse landscape of India. Such an investigation is also likely to benefit researchers interested in characterising vegetation phenology.

The objective of the present research was to compare four models (Fourier, asymmetric Gaussian, double logistic and Whittaker smoother) for representing time-series VI data to support the estimation of phenological parameters. The focus was on finding the model(s) which (a) reproduce discernible phenological patterns adequately while (b) being robust to random temporal fluctuations.

Fourier analysis is a common method for smoothing time-series satellite sensor data because it has only one model parameter (i.e., number of harmonics) to achieve the required degree of smoothing, and the Fourier algorithm can be implemented readily with a few lines of software code. Geerken (2009) revealed the usefulness of different Fourier harmonics to monitor seasonal and inter-annual changes in vegetation phenology. Several studies have reported the utility of the Asymmetric Gaussian and Double Logistic models over other fitting techniques and filters (Beck et al., 2006; Hird & McDermid, 2009; Jönsson & Eklundh, 2002, 2004). Vilela et al. (2007) utilised the Whittaker smoother (Eilers, 2003) to extract the desired signal from metabolic profiles obtained from *in-vivo* NMR data with a non-stationary noise structure and also revealed that it performs slightly more accurately than the Savitzky–Golay filter. Recently, the Whittaker smoother was utilised to smooth 10 years of 10-daily SPOT VGT data covering South America (Atzberger & Eilers, 2011a).

The present research aimed to analyse the above four models for smoothing temporal satellite sensor observations with the purpose of estimating phenological parameters. A comparative analysis of the capability and reliability of these techniques is provided. We chose the vegetated landscape of India for this comparison because of its diversity and spatial heterogeneity, and a developing interest in mapping its phenology.

2. Methods

Fig. 1 presents a schematic diagram of the steps and processes followed in the research. Overall, there are four major components: database creation, smoothing, phenology estimation and evaluation. Database creation is described in Section 2.2. The time-series was smoothed by fitting four models to the local mean: Fourier, asymmetric Gaussian, double logistic and the Whittaker filter. The following sections provide a detailed description of each of the models.

2.1. Fourier analysis

A complex vegetation growth cycle over a given temporal period can be expressed using Fourier analysis as the sum of a series of cosine waves and a constant term (Jakubauskas et al., 2001; Wagenseil &

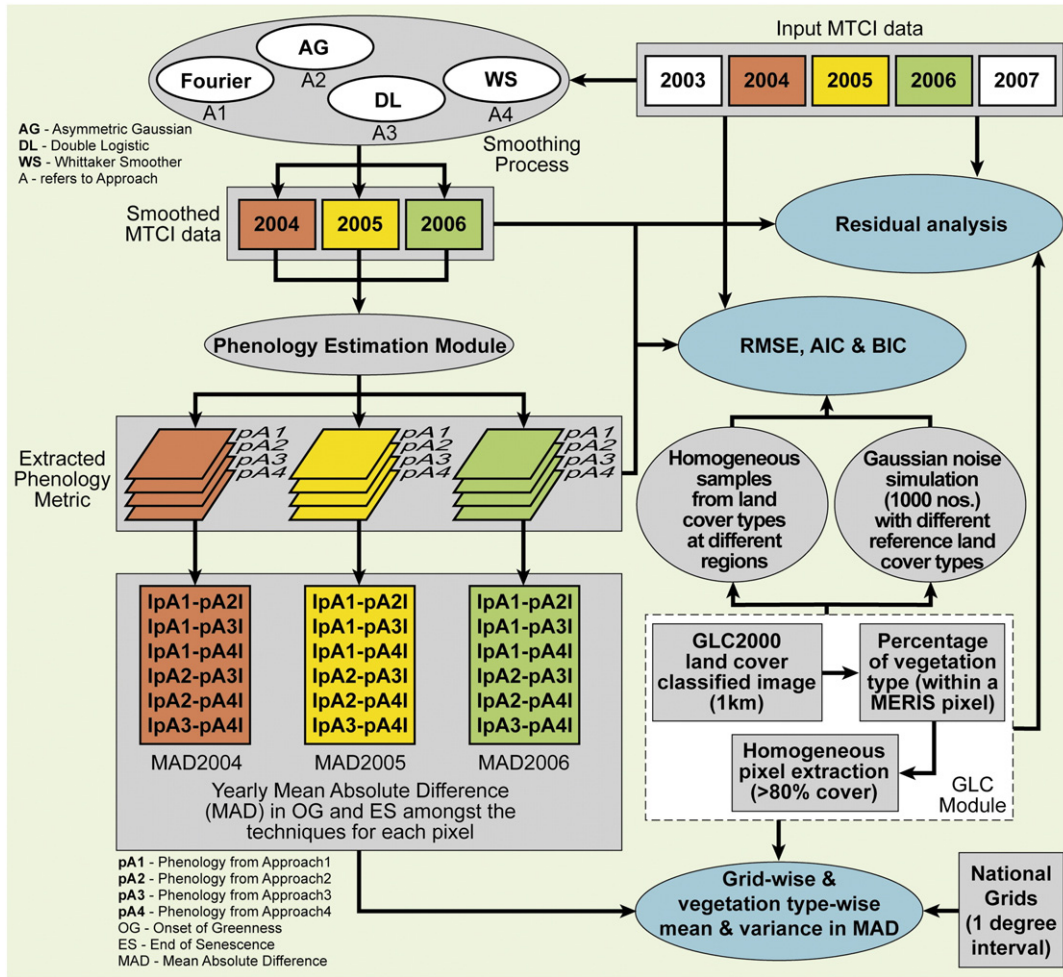


Fig. 1. Schematic diagram representing the processing steps undertaken in this research.

Samimi, 2006). Fourier analysis decomposes the vegetation temporal profile into a series of sinusoids of different frequency. Individual sinusoids and their frequencies (i.e., harmonics) can be amalgamated into a complex waveform, closely resembling the input vegetation profile, for which “noise” has been removed.

The Discrete Fourier Transform is given by:

$$F_{(u)} = \frac{1}{N} \sum_{t=0}^{N-1} VI(t) * e^{-2\pi i u t / T} \quad (1)$$

where $VI(t)$ is the input vegetation index value at time t in the time-series, u is the number of Fourier components, t is the composite number, T is the length of time period (number of composites), and here T is equal to N , the number of data in the time-series. The above equation consists of two parts: cosine (real, $F_{C(u)}$) and sine (imaginary, $F_{S(u)}$), where the cosine part is:

$$F_{C(u)} = \frac{1}{N} \sum_{t=0}^{N-1} \left(VI(t) * \cos\left(2\pi \frac{u t}{T}\right) \right) \quad (2)$$

and the sine part is

$$F_{S(u)} = \frac{1}{N} \sum_{t=0}^{N-1} \left(VI(t) * \sin\left(2\pi \frac{u t}{T}\right) \right) \quad (3)$$

Using Eqs. (2) and (3), the Fourier magnitude (F_m) can be calculated as

$$F_{m(u)} = \sqrt{F_{C(u)}^2 + F_{S(u)}^2} \quad (4)$$

and the phase (F_p) can be calculated as

$$F_{p(u)} = a \tan 2 \left(\frac{F_{C(u)}}{F_{S(u)}} \right) \quad (5)$$

In Fourier analysis, high frequency noise fluctuations are filtered out and lower frequency harmonics are interpreted as representing the dominant seasonal variation in the vegetation index (Wagenseil & Samimi, 2006). Utilising the estimated parameters, a smoothed set of data can be reconstructed (i.e., $VI^*(t)$) as per Eq. (6).

$$VI^*(t) = F_{m(0)} + \sum_{n=1}^u F_{m(n)} \cos\left(\frac{2\pi n t}{T} - F_{p(n)}\right) \quad (6)$$

Hence, by utilising an appropriate number of harmonics (u) the phenological information present in the time-series can be better assessed.

To implement Fourier-based smoothing, a software routine was developed under ARCGIS using Arc-objects and Visual Basic (Dash et al., 2010).

2.2. Global fitting through embedded local functions

A global function representing the complex behaviour in phenological variation over the growing season can be constructed by merging a set of local functions (Jönsson & Eklundh, 2004). For the time-series data represented in Fig. 2 the global function $VI^*(t)$ over the time interval $[t_L, t_R]$ can be written using functions representing the local time-series variation around the left minima, $f_L(t)$, the central maxima, $f_C(t)$ and the right minima, $f_R(t)$, as

$$VI^*(t) = \alpha(t)f_L(t) + [1 - \alpha(t)]f_C(t), \quad t_L < t < t_C \\ = \beta(t)f_C(t) + [1 - \beta(t)]f_R(t), \quad t_C < t < t_R \quad (7)$$

where $\alpha(t)$ and $\beta(t)$ are cut-off functions around the short temporal interval $(t_L + t_C)/2$ and $(t_C + t_R)/2$, respectively, smoothly decreasing from 1 to 0.

A local function takes the form

$$f(t) \equiv f(t; c_1, c_2, a_1, a_2, \dots, a_n) \equiv c_1 + c_2 g(t; a_1, a_2, \dots, a_n) \quad (8)$$

where $g(t; a_1, a_2, \dots, a_n)$ represents the basis function for fitting the given data points and c_1, c_2 represent the base level and amplitude, respectively. For a given set of data points in an interval around a maximum or minimum, the parameters c_i and a_i are estimated by minimising

the merit function using a Levenberg–Marquardt method (Jönsson & Eklundh, 2006).

2.2.1. Asymmetric Gaussian function

The asymmetric Gaussian (AG) function (Jönsson & Eklundh, 2002) can be used as a basis function, and written as

$$g(t; a_1, a_2, \dots, a_5) = \exp\left[-\left(\frac{t-a_1}{a_2}\right)^{a_3}\right], \quad t > a_1 = \exp\left[-\left(\frac{a_1-t}{a_4}\right)^{a_5}\right], \quad t < a_1 \quad (9)$$

where, $g(t; a_1, a_2, \dots, a_5)$ is the Gaussian-type fit function, a_1 is related to position (in time) of the minimum or maximum, a_2 and a_3 are related to the width and flatness of the right half function, and a_4 and a_5 are related to the width and flatness of the left half function.

2.2.2. Double logistic function

The double logistic (DL) function (Beck et al., 2006; Zhang et al., 2003) can be used as a basis function, written as

$$g(t; a_1, \dots, a_4) = \frac{1}{1 + \exp\left(\frac{a_1-t}{a_2}\right)} - \frac{1}{1 + \exp\left(\frac{a_3-t}{a_4}\right)} \quad (10)$$

where, a_1 and a_3 determine the position of the left and right inflection points of the curve, respectively, and a_2 and a_4 determine the rate of change at the left and right inflection points, respectively.

The TIMESAT software (Jönsson & Eklundh, 2004) was used to fit the AG and DL models.

2.3. Whittaker smoother

The ‘Whittaker smoother’ (Atzberger & Eilers, 2011a,b; Eilers, 2003) is based on penalised least squares. It fits a discrete series to discrete data and penalises the roughness of the smooth curve. In this way, it balances reliability of the data and roughness of the fitted data. The smoother the result, the more it will deviate from the input data. A balanced combination of the two goals is the sum (Q):

$$Q = S + \lambda R \quad (11)$$

with

$$S = \sum_t (VI(t) - VI^*(t))^2 \quad (12)$$

$$R = \sum_t (VI^*(t) - 3VI^*(t-1) + 3VI^*(t-2) - VI^*(t-3))^2. \quad (13)$$

The lack of fit to the data S is measured as the usual sum of squares of differences (Eq. 12). The roughness of the smoothed curve R is expressed here as third order differences (Eq. 13). The smoothing parameter λ is chosen by the user. The aim of penalised least squares is to find the series $VI^*(t)$ that minimises Q . The larger the parameter λ , the greater is the influence of R on the goal Q and the smoother will be $VI^*(t)$ (at the cost of the degradation of the fit).

Eilers (2003) showed that λ can be determined using cross-validation. Cross-validation involves leaving out each of the non-missing elements of $VI(t)$ in turn, smoothing the remaining data and predicting $VI^*(t)$ for each omitted value. By repeating this for all $VI(t)$ of length N the cross-validation standard error can be computed and the most appropriate smoothing parameter selected. Another way of choosing a value for the smoothing parameter λ is to tune it until a visually pleasing result is obtained (Eilers, 2003).

Based on previous experience with a large SPOT VGT data set covering South America (Atzberger & Eilers, 2011a), it was decided not to use the automatic but time consuming optimization procedure, but to run the smoother with two contrasting values for λ (i.e., $\lambda = 2$ and 15). With $\lambda = 15$ a very smooth curve is obtained, which is suitable

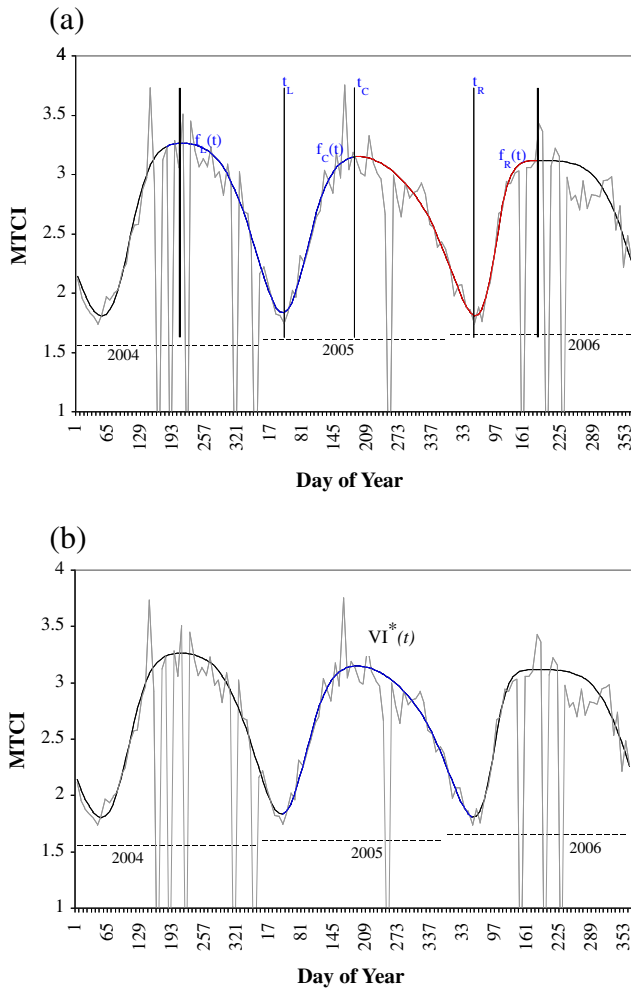


Fig. 2. Graphical illustration of deriving a global function using a set of local functions. (a) Local functions for left $f_L(t)$, central $f_C(t)$ and right $f_R(t)$ parts and (b) global function $VI^*(t)$ over the time interval $[t_L, t_R]$. The grey line indicates the noisy input MTCI data and the smooth line indicates the fitted local basis function.

for most conditions, while with $\lambda=2$ more weight is given to the original data allowing, for example, characterisation of a double cropping system.

The Whittaker smoother was implemented under Matlab, using function files provided by Eilers (2003) and assuming a white (un-biased) noise distribution.

3. Study area and data

3.1. Study area

The whole of India was selected as a suitable study site for this research because of its diversity. The Indian sub-continent is enriched with vegetation spreading over Central India, the Eastern and Western Ghats in the south, the Eastern Himalayas in the north-east and Western Himalayas in the north. Of the total geographical area (≈ 328 million ha) of the country, 69.09 million ha (21.02%) constitutes forest cover from which 8.35 million ha (2.54%) is very dense, 31.90 million ha (9.71%) is moderately dense and 28.84 million ha (8.77%) is open forest (SFR, 2009). The types of natural vegetation cover include tropical and sub-tropical evergreen forests, tropical semi-evergreen forest, tropical moist and dry deciduous forests, tropical thorn forest, temperate conifer forest, temperate broad leaved forest, temperate mixed forest, sub-alpine forest, mangrove forest, alpine meadows and grasslands (Joshi et al., 2006).

3.2. Data

Temporal (8-day) composites of MERIS MTCI data (level-3 product) for the period 2003 to 2007 were acquired for the whole of India. Data were obtained from the Natural Environment Research Council (NERC) Earth Observation Data Centre (NEODC) (<http://www.neodc.rl.ac.uk/>) (supplied by ESA and processed by Infoterra Ltd). The MTCI level-3 product has a spatial resolution of 4.6 km and contains 46 composites per year. MTCI was utilised in this research, in preference to other vegetation indices (such as the NDVI and EVI), because of its greater correlation with canopy chlorophyll content and limited sensitivity to atmospheric effects, soil background and view angle (Dash & Curran, 2007).

The MTCI is calculated as in Eq. (14) using wavebands at 753.75 nm, 708.75 nm and 681.25 nm referred to as respectively as R_{band10} , R_{band9} , and R_{band8} .

$$\text{MTCI} = \frac{R_{\text{band10}} - R_{\text{band9}}}{R_{\text{band9}} - R_{\text{band8}}} \quad (14)$$

Each composite represents approximately 8 days and is referred to by a composite number (CN).

4. Processing

4.1. Phenology extraction

4.1.1. Pre-processing

Cloud cover is prominent in most regions of India during the monsoon season (June–September) and this resulted in numerous dropouts in the images. Besides data dropouts, we also observed some errors due to undetected clouds and poor atmospheric conditions which occurred throughout the entire annual growing cycle. Different approaches to eliminating these sources of errors and dropouts were adopted for each model. For the AG and DL models (under the TIMESAT software), errors were identified using a standard deviation threshold and then eliminated through a temporal median filter. In Fourier analysis, as used in the present study, dropouts were eliminated through an averaging process, which considers a temporal neighbourhood of available data on both sides of a dropout value,

with a temporal moving window of size ranging from a week up to two months (see Dash et al., 2010 for details). The Whittaker filter smoothes the data directly without any pre-processing.

After removing obvious errors, the data were fitted with each of the models: Fourier, AG, DL and Whittaker filter. In the Fourier method, each year of data was fitted independently, whereas the entire time series (2003–2007) was filtered in a single run using the Whittaker smoother. A minimum of three years of data is required for the TIMESAT software (AG and DL models). Hence, the data from 2003 to 2007 were used to fit the AG and DL models and then the results for 2004 to 2006 were utilised in the comparative analysis.

4.1.2. Exploring model parameters

The landscape of India is diverse and complex, and the agricultural field sizes are generally small. Moreover, the vegetated landscape encompasses natural and human-managed vegetation with both single and double annual growing seasons, and even three annual crop growing patterns in some agricultural regions. Hence, finding a single set of model parameters for any of the four tested models that is appropriate across the whole country was challenging. The ability of each of the four models to represent faithfully a set of annual seasonal cycles was analysed, using different fitting criteria, over different land cover types and for several dominant vegetation types.

While experimenting with the four models over India it was revealed that two major vegetation landscapes (i.e., natural vegetated landscape and agricultural landscape) influenced most strongly the model fitting: natural vegetation has a single annual growth pattern while most of the agricultural practices in India follow a double cropping pattern. In the Fourier approach, the natural vegetation growth cycle (i.e., single season) could be fitted reliably using the first three or four Fourier components (i.e., mean + 3 harmonics), but for agricultural landscapes (i.e., double or triple season) six Fourier components (i.e., mean + 5 harmonics) were required (Dash et al., 2010; Jeganathan et al., 2010a,b).

The parameters for the DL and AG models were adjusted interactively in the TIMESAT software to arrive at closely fitting results. In TIMESAT, a seasonality parameter value of between 0.1 and 0.7 was used for fitting the double season profiles (i.e., agricultural landscapes) and larger values (> 0.7) were used for single seasons. The Median filter option with a parameter value of 2 was chosen to remove spikes or noise as it was suitable for both landscape types. Instead of fitting to the upper envelope (which is normally done with NDVI data to avoid atmospheric attenuation) the medium envelope (value = 2) was chosen and the adaptation strength of fitting was kept at the value of 2 while maintaining the fitting accuracy.

The Whittaker filter was applied with two different settings of λ ($\lambda = 2$ and $\lambda = 15$). A value of $\lambda = 2$ fitted the data more closely, but was very sensitive to minute fluctuations. $\lambda = 2$ is well suited to fitting double season profiles. On the other hand $\lambda = 15$ provided the annual smooth trend, suitable for all natural vegetation growth cycles (i.e., single season). It could be argued that $\lambda = 15$ provides a generally acceptable fitting across all cases, but $\lambda = 2$ is included here because it is illustrative of the capabilities of the Whittaker filter about which less is known in the remote sensing community.

4.1.3. Estimation of vegetation onset and senescence

After smoothing, two phenological parameters (e.g., onset of greenness, OG, and end of senescence, ES) were estimated using an iterative search process over the annual smoothed data. This process considers increasing or decreasing trends in the MTCI values of successive temporal neighbours (8 days). Onset of greenness was defined as a valley point at the beginning of a growing cycle, and end of senescence was defined as a valley point occurring at the decaying end of a phenology cycle. The algorithm starts from the dominant peaks and searches both forwards and backwards in time checking the derivative information. While moving backwards, a change in derivative value from

positive to negative may indicate a valley point, while moving forward, a change in derivative from negative to positive may indicate a valley point (see Dash et al., 2010 for details). Logical and continuity functions were implemented to identify false detection of OG and EG due to local fluctuations. The OG and ES time points were chosen as the nearest composite date at which the valley point occurs. The phenology parameters (OG and ES) were estimated using the same approach for all data. However, only OG was analysed and compared between all the models.

4.2. Model evaluations at different levels of homogeneity

The smoothed data and phenological parameters estimated from each fitted model were evaluated (within different vegetation types, regions and years) using different measures at the sample level, pixel level and at an aggregated level. The approach is illustrated in Fig. 1.

The global land cover map, GLC2000 (Bartholome & Belward, 2005; Stibig et al., 2007), with a spatial resolution of 1 km was used (i) to identify homogeneous (> 80% cover) vegetated pixels of MERIS and (ii) to identify reliable sample pixels for different vegetation classes. Homogeneity was calculated using a block statistical function which identifies the percentage of vegetative class pixels falling within a MERIS pixel. Pixels with 80% to 100% vegetation cover were extracted as representative homogeneous pixels. In India, evergreen, semi-evergreen, moist deciduous and dry deciduous vegetation types constitute a major proportion of all natural vegetation and, hence, only the homogeneous pixels from these four vegetation types were considered for further analysis.

At the sample level, representative sample points were collected from different vegetation types, in different years, occurring in different regions. Sample pixels were identified carefully from major vegetation types with homogeneous cover in different regions to avoid edge or mixed pixels when analysing the effect of fitting. At the pixel level, the models were fitted to data for each pixel in the study area. At the aggregated level, analysis was undertaken with two different approaches. First, model performance was evaluated over a set of homogeneous pixels stratified by vegetation type. The analysis was restricted to homogeneous pixels with more than 80% vegetative cover to provide reliable reference annual profiles. Secondly, the model results at the pixel level were aggregated to 1 × 1 grid cells to reveal broader deviations in the results for each model.

To find meaningful patterns in the differences in OG between the four models, the OG results were compared with one another. The absolute difference in OG between each model was calculated for each pixel. This differencing process yielded six difference images (i.e., |AG – DL|, |AG – FT|, |AG – WH|, |DL – FT|, |DL – WH|, |FT – WH|). The absolute difference in the parameters between pairs of models and the mean absolute difference (MAD) between all the models were calculated for every year and every pixel. Then, the mean and variance of the MAD were calculated for the pixels falling within each of the 1° × 1° grid cells to characterise the spatial pattern of the difference. The differences within the homogeneous pixels from major vegetation types were also estimated.

4.3. Performance measures

The statistical evaluation measures used in this study were: root mean square error (RMSE) (Eq. 15) residual error (RE) (Eq. 16), Akaike Information Criterion (AIC) (Eq. 17) and Bayesian Information Criterion (BIC) (Eq. 18). For model ranking, a performance count i.e., a count of how many times a particular model outperformed the others, was estimated by inter-comparing the superiority of model results in terms of RMSE, AIC and BIC values for each input.

The RMSE was calculated for each pixel between the original (observed) data and fitted data and also for homogeneous pixels

(≥80% vegetative cover) for the four major vegetation types in India. For the residual error (RE), the smoothed values over homogeneous pixels were compared with the observed values at each temporal point. The residuals for homogeneous pixels only were extracted and then the mean residual value and 95% confidence interval were plotted for comparison.

$$\text{RMSE} = \left(N^{-1} \sum_{t=1}^N (\text{VI}^*(t) - \text{VI}(t))^2 \right)^{1/2} \quad (15)$$

$$\text{RE}(t) = [\text{VI}^*(t) - \text{VI}(t)] \quad (16)$$

4.3.1. Akaike Information Criterion (AIC)

The performance of a fitted model depends largely on the number of free parameters (the effective dimension) of the model. The AIC (Akaike, 1973) can be used to measure the effective performance of a model by penalising for a large number of parameters. Hence, we adopted the AIC to evaluate the performance of the fitting techniques. AIC is calculated using Eq. (17).

$$\text{AIC} = 2k + n[\ln(\text{RSS})] \quad (17)$$

where, k is the number of free parameters in the model, n is the number of input data points and RSS is the residual sum of squares between the original data and fitted model. A lower value of AIC would indicate the preferable model.

Two parameters (i.e., magnitude, F_m and phase, F_p) are required for every Fourier component (Eq. 6) and hence k for Fourier-based fitting was equal to seven (i.e., mean + (3 harmonics × 2) = 7) for a single season vegetation growth cycle. For the AG model (Eq. 9) seven parameters are needed (i.e., $a_1, a_2, a_3, a_4, a_5, c_1$ and c_2), and for the DL model (Eq. 10) six parameters are required (i.e., a_1, a_2, a_3, a_4, c_1 and c_2). For the Whittaker smoother, the effective dimension corresponds to the trace of the hat matrix (Eilers & Marx, 1996), which depends on the selected value of the roughness parameter (λ) and number of observations. For $\lambda = 2$ the effective dimension, which is non-integer and closely related to number of parameters, is 18.84, and it is 9.37 when $\lambda = 15$.

4.3.2. Bayesian Information Criterion (BIC)

The Bayesian information criterion (BIC) (Schwarz, 1978) is another measure of goodness-of-fit, similar to the AIC, but using a Bayesian framework. It is calculated using Eq. (18).

$$\text{BIC} = n \left(\ln \left[\hat{\sigma}^2 \right] \right) + k \cdot \ln(n) \quad (18)$$

where $\hat{\sigma}^2$ is the error variance and k and n have a similar meaning to that in the AIC. BIC is similar to the AIC, but also adjusts for sample size. It generally penalises free parameters more strongly than does AIC.

4.4. Evaluating the effect of noise on model fitting

To characterise the robustness of each technique to noise, randomly drawn noise realisations (from a Gaussian distribution) were added to an observed vegetation profile. The noisy datasets were fitted with each model, and the fitted values checked against the reference mean annual profile to derive the RMSE, AIC and BIC. A performance count was used to identify the model which consistently yielded the smallest values of RMSE, AIC and BIC.

For each of the four major vegetation types 1000 noisy data sets were simulated. For each vegetation type, homogeneous pixels with more than 80% vegetation cover were identified as mentioned in Section 4.2. A representative mean and standard deviation of the MTCL values at each time composite was calculated from the “pure”

pixels, independently for each vegetation type. This also yielded a representative mean annual reference profile for each vegetation type

$$\tilde{y}_t \sim N(\mu_t, \sigma_t^2) \quad (19)$$

where t represents a time composite. Each of the 1000 data sets contains 46 time composites of noisy data (i.e., noise added to a representative mean annual profile).

5. Results

The temporal MTCI patterns were directly related to seasonal changes in vegetation growth. The MTCI values increased during the greening phase and diminished during the senescence phase in

relation to the canopy integrated chlorophyll content. Over India, the largest MTCI values (annual maxima) ranged between 3.5 and 4 for dense natural vegetation and were as large as 4 to 4.5 for high-yield agricultural crops. For non-vegetated areas the MTCI values remained close to 1 which is the smallest reference value.

5.1. Non-spatial evaluation of fitting techniques

Fig. 3 presents the four fitted models (four harmonics for Fourier analysis; $\lambda = 15$ for Whittaker) along with the original MTCI data collected at different sample locations. These figures facilitate visual assessment. Fig. 3 provides the fitting results for the year 2006 for the tropical evergreen pixels located in Arunachal Pradesh in the north-eastern region (Fig. 3a) and in the Western Ghats area in Kerala

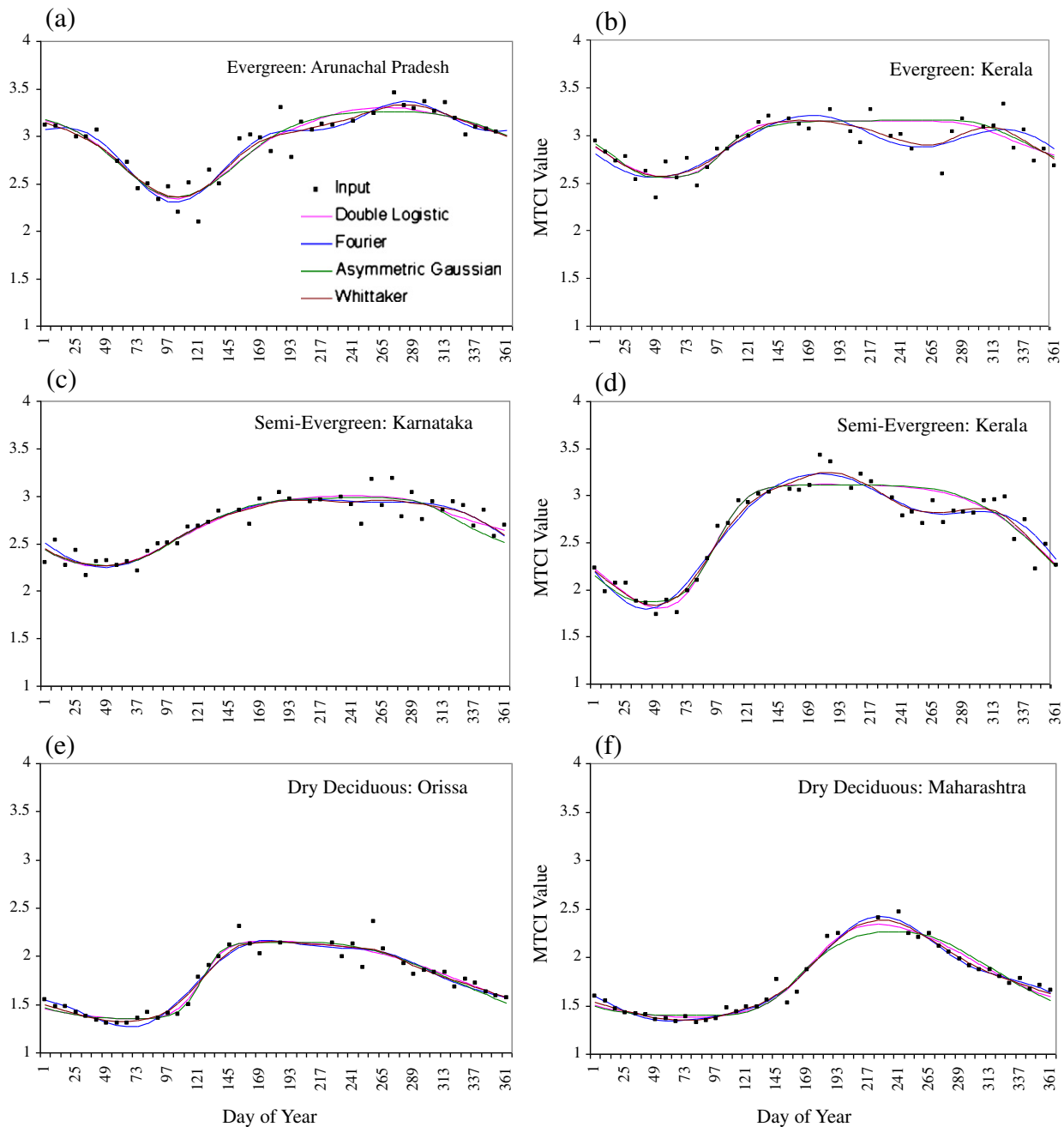


Fig. 3. Four models fitted to time-series acquired from homogeneous pixels of three different vegetation types in different regions of India in 2006. [Evergreen vegetation from (a) Arunachal Pradesh and (b) Kerala; semi-evergreen vegetation from (c) Karnataka and (d) Kerala; dry deciduous vegetation from (e) Orissa and (f) Maharashtra].

in the south-western region (Fig. 3b) of India. Similarly, the fitted models for the semi-evergreen, and dry deciduous vegetative pixels located in Karnataka and Kerala, and Maharashtra and Orissa are depicted in Fig. 3c&d, and e&f, respectively. The variation in the growth rhythm and associated fitting results for moist deciduous vegetation types sampled at Karnataka and Orissa (over the years 2004 to 2006) are shown in Fig. 4. The coordinates of the sample locations are: evergreen (Arunachal Pradesh 27° 40' 27.80" N, 96° 04' 01" E; Kerala 9° 39' 54" N, 77° 03' 34" E), semi-evergreen (Karnataka 12° 47' 04" N, 75° 31' 14" E; Kerala 9° 02' 28" N, 77° 01' 04" E); moist deciduous (Karnataka 13° 49' 27" N, 75° 51' 12" E; Orissa 21° 51' 05" N, 86° 27' 33" E); dry deciduous (Orissa 18° 31' 27" N, 82° 10' 31" E; Maharashtra 21° 46' 06" N, 73° 53' 54" E).

Fig. 5 presents the results for the sample agricultural pixels in different regions of India revealing both double and triple cropping seasons for the year 2004. It was observed that the DL and AG models were affected by local fluctuations in the data as well as by the data trend in the pre- and post-temporal point sequence (i.e., falling in the previous or next year's cycle), which is clear in the fitting results for the evergreen and semi-evergreen samples.

Table 1 presents the RMSE values for the major vegetation types from different regions and years (as referred to in Fig. 3 for the year 2006). The smallest RMSE values indicate a close fit. It can be seen readily that the Whittaker model ($\lambda = 15$) performed consistently more accurately than all other models, followed by the Fourier model in most cases. However, the fitted model is expected to reveal the

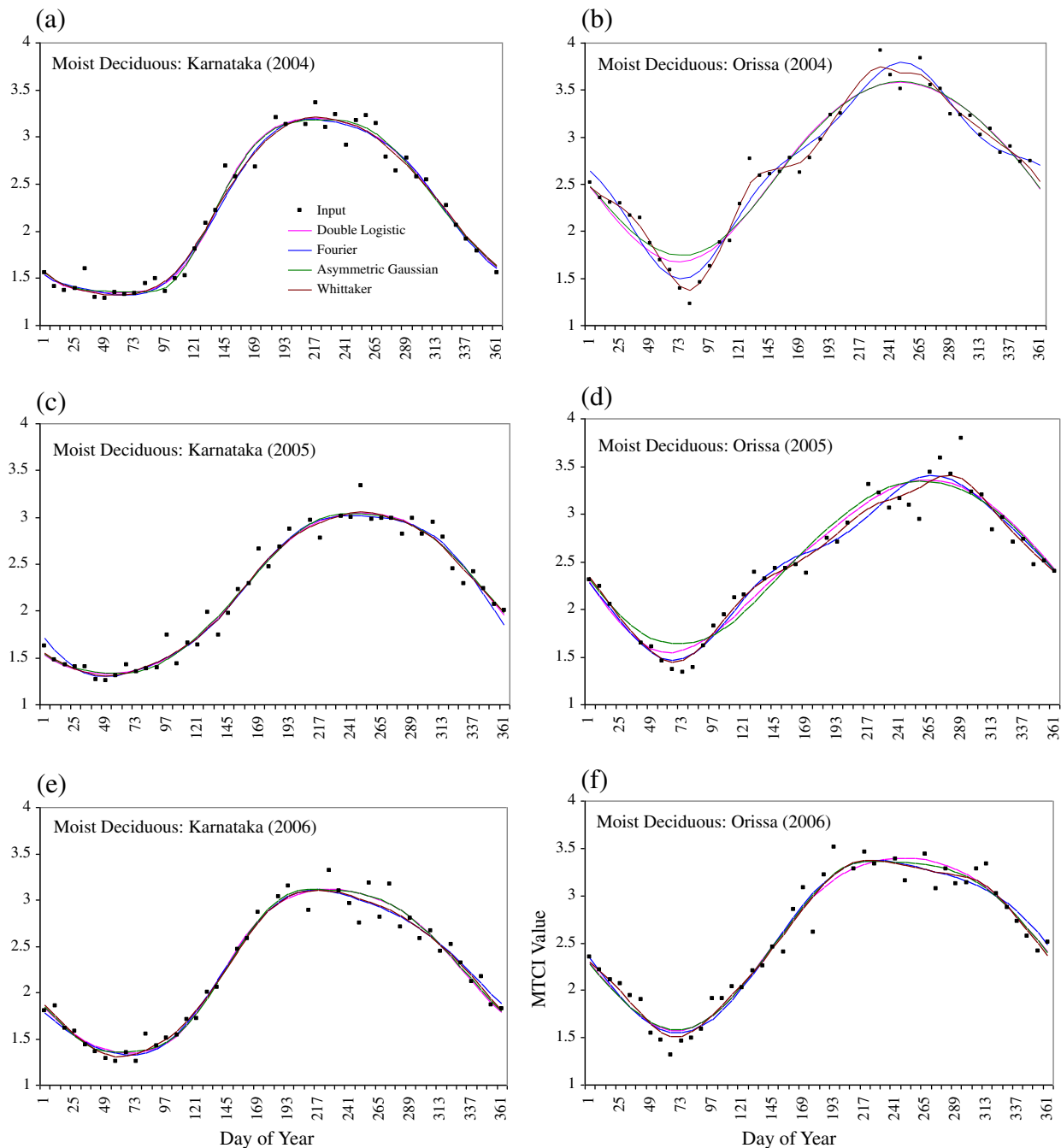


Fig. 4. Four models fitted to time-series acquired from homogeneous pixels of moist deciduous vegetation from the (a,c,e) Karnataka and (b,d,f) Orissa states of India in the years (a, b) 2004, (c,d) 2005 and (e,f) 2006 derived using four different fitted models.

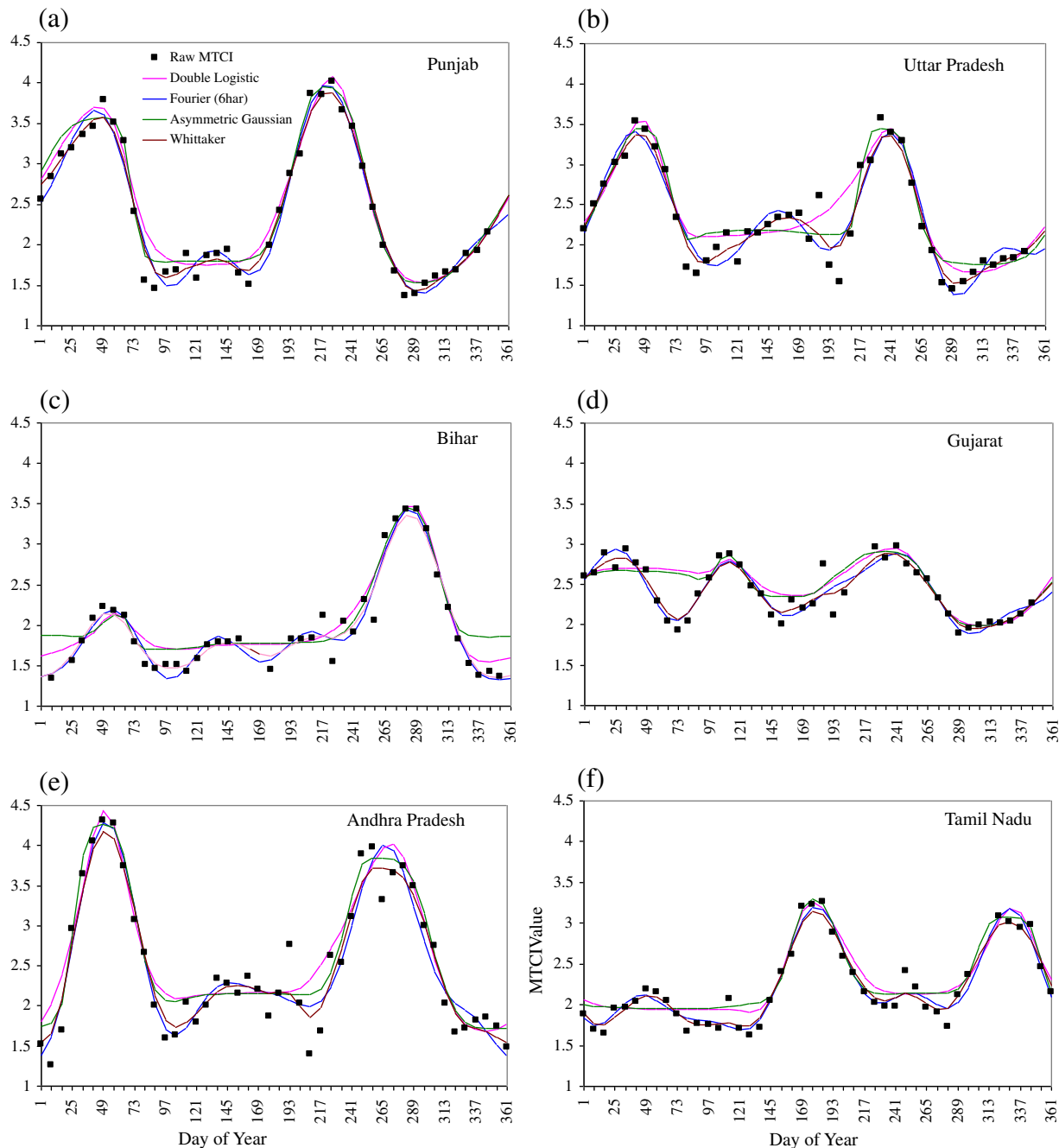


Fig. 5. Four models fitted to time-series acquired from homogeneous pixels of agricultural crops from (a) Punjab, (b) Uttar Pradesh, (c) Bihar, (d) Gujarat, (e) Andhra Pradesh, and (f) Tamil Nadu.

major annual phenological pattern while being robust to local random noise. Hence, the RMSE or any other simple distance measure is not a suitable performance indicator in isolation because by simply increasing the number of parameters of a model one can increase accuracy arbitrarily. Hence, the fitted models were evaluated further using the AIC and BIC. Table 1 also presents the RMSE, AIC and BIC for the fitted models from 24 different samples (two samples each for four vegetation types over three years) distributed over four vegetation types in different regions in different years (the fitting results for the year 2006 are shown in Fig. 3; the results for all years were analysed and evaluation measures are provided for each sample datum in Table 1). The smaller the RMSE, AIC and BIC, the better is the fit. The model with the smallest score in each row is highlighted in bold.

Finally, performance count (a count of how many times a particular model outperformed the others) was calculated for each model. It was found that the Whittaker smoother outperformed all other models if the RMSE and AIC were chosen as the deciding criteria. Under BIC, the performance counts of the Fourier and Whittaker approaches were equal. Overall, the Whittaker filter outperformed the others. The Fourier approach was preferable to the DL and AG models in all three evaluation scenarios. The AG model acquired zero score under the AIC, but for the BIC it scored more than the DL model. Figs. 3 to 5 reflect the close fitting of the Whittaker and Fourier approaches. The DL and AG models were accurate for moist deciduous vegetation types and hence yielded competitive results for AIC and BIC (Table 1) compared to the Fourier and Whittaker approaches.

Table 1

Root mean square error (RMSE), Akaike Information Criterion (AIC) and Bayesian Information Criterion (BIC) based assessment of four fitting models (Double Logistic–DL, Asymmetric Gaussian–AG, Fourier–FT, Whittaker–WH) at the sample locations shown in Figs. 3 and 4 (in bold, best fitting models).

Fitting results		RMSE				AIC				BIC			
Vegtype (year)	Location	DL	AG	FT	WH	DL	AG	FT	WH	DL	AG	FT	WH
Evergreen (2004)	Arunachal Pradesh	0.144	0.145	0.117	0.114	2.61	5.51	−16.12	−12.33	−113.32	−116.00	−134.04	−127.08
Evergreen (2004)	Kerala	0.102	0.113	0.092	0.087	−20.04	−7.40	−26.43	−26.72	−140.37	−133.34	−148.75	−145.82
Evergreen (2005)	Arunachal Pradesh	0.128	0.128	0.126	0.115	−1.59	0.36	−1.09	−4.08	−126.36	−130.04	−127.85	−127.57
Evergreen (2005)	Kerala	0.232	0.203	0.142	0.136	48.97	40.23	6.16	9.79	−89.29	−103.74	−134.10	−127.04
Evergreen (2006)	Arunachal Pradesh (Fig. 3a)	0.116	0.120	0.104	0.106	−9.07	−4.83	−15.42	−9.99	−138.31	−139.73	−146.66	−137.89
Evergreen (2006)	Kerala (Fig. 3b)	0.142	0.141	0.125	0.110	−0.15	3.55	−10.67	−16.23	−129.39	−131.35	−140.24	−144.14
Semi-evergreen (2004)	Karnataka	0.111	0.110	0.111	0.094	−15.18	−13.85	−12.73	−21.95	−148.91	−153.27	−148.46	−154.31
Semi-evergreen (2004)	Kerala	0.146	0.143	0.142	0.132	10.25	10.84	9.84	7.68	−128.02	−133.14	−130.42	−129.16
Semi-evergreen (2005)	Karnataka	0.109	0.109	0.106	0.096	−14.52	−12.50	−15.31	−20.17	−157.34	−161.06	−160.13	−161.52
Semi-evergreen (2005)	Kerala	0.152	0.156	0.134	0.129	14.76	18.35	4.62	5.64	−141.89	−144.11	−154.03	−149.40
Semi-evergreen (2006)	Karnataka (Fig. 3c)	0.104	0.111	0.102	0.099	−20.39	−17.19	−21.12	−19.61	−163.20	−165.74	−165.94	−160.96
Semi-evergreen (2006)	Kerala (Fig. 3d)	0.145	0.152	0.119	0.102	7.20	13.33	−13.89	−21.10	−140.20	−139.83	−163.29	−166.99
Moist deciduous (2004)	Karnataka (Fig. 4a)	0.101	0.102	0.105	0.101	−19.10	−16.95	−14.26	−14.07	−157.36	−160.93	−154.52	−150.90
Moist deciduous (2004)	Orissa (Fig. 4b)	0.182	0.187	0.134	0.116	27.92	32.29	5.42	−3.81	−110.34	−111.69	−134.84	−140.65
Moist deciduous (2005)	Karnataka (Fig. 4c)	0.105	0.108	0.109	0.100	−17.76	−13.83	−14.83	−16.21	−169.77	−171.62	−168.84	−166.66
Moist deciduous (2005)	Orissa (Fig. 4d)	0.162	0.181	0.145	0.117	18.35	30.47	11.64	−2.26	−124.47	−118.09	−133.17	−143.60
Moist deciduous (2006)	Karnataka (Fig. 4e)	0.111	0.108	0.107	0.102	−14.21	−14.08	−14.98	−15.42	−157.03	−162.64	−159.80	−156.76
Moist deciduous (2006)	Orissa (Fig. 4f)	0.144	0.140	0.139	0.123	8.84	7.81	6.04	0.41	−138.57	−145.35	−143.36	−145.47
Dry deciduous (2004)	Orissa	0.089	0.102	0.084	0.068	−30.74	−16.93	−34.96	−48.51	−173.56	−165.49	−179.77	−189.86
Dry deciduous (2004)	Maharashtra	0.104	0.109	0.103	0.097	−16.91	−11.70	−15.81	−16.68	−150.64	−151.12	−151.55	−149.03
Dry deciduous (2005)	Orissa	0.093	0.093	0.086	0.075	−28.46	−26.58	−32.57	−41.15	−175.87	−179.74	−181.98	−187.03
Dry deciduous (2005)	Maharashtra	0.083	0.086	0.083	0.079	−37.17	−33.39	−37.17	−35.54	−175.43	−177.36	−177.43	−172.37
Dry deciduous (2006)	Orissa (Fig. 3e)	0.075	0.075	0.082	0.076	−43.28	−42.45	−34.76	−36.72	−177.01	−181.87	−170.50	−169.07
Dry deciduous (2006)	Maharashtra (Fig. 3f)	0.063	0.080	0.053	0.054	−61.14	−39.84	−72.78	−67.68	−199.40	−183.82	−213.04	−88.80
Performance count		0	0	2	22	5	0	7	13	2	4	9	9

Although the AIC and BIC are influenced by the fitting errors (i.e., residual sum of squares, RSS, and fitting variance, between the model and the data), these measures also integrate the number of free parameters. The number of free parameters compensated for the larger fitting error, which can be seen in Table 1 (e.g., through the first two rows, representing evergreen in year 2004, where the Fourier method resulted in a larger RMSE than the Whittaker filter, but performed better in terms of the AIC and BIC; through the third row where AG had the largest error, but performed better in terms of BIC). Overall, the Whittaker and Fourier approaches emerged consistently as the most suitable models, in terms of RMSE, AIC and BIC.

Fig. 4 provides the temporal variation in the growth rhythm of moist deciduous vegetation and the fitting results for different years. The performance results of the fitted models in Fig. 4 are also provided in Table 1. Fig. 5 presents the fitting results for samples over agricultural areas from Punjab, Uttar Pradesh, Bihar, Gujarat, Andhra Pradesh and Tamil Nadu in the year 2004 (six harmonics for Fourier and $\lambda = 2$ for Whittaker). It was found that the AG and DL models did not provide a satisfactory fit when there was more than one growing season. Since the main parameter governing the AG and DL fit is the slope of the growth curve, the fitting was more accurate at sloping regions and, thus, the required OG and ES points were not identified appropriately. Also noise in-between two growing seasons affected the fitting results more in the AG and DL models than in the Fourier and Whittaker approaches.

For natural vegetation, flat peaks of long duration are unlikely in the growing season. Both the AG and DL models enforce a single peak irrespective of the duration of the flatness at the peak and, hence, do not consider minor fluctuations even though a natural system is being represented. However, these two techniques maintain the slopes adequately during the greening and decaying phases. The Fourier fitting is not affected by scattered noise values which deviate positively from the annual trend, but is influenced by negative bias and natural oscillations and, hence, sometimes results in an undulating pattern (e.g., Figs. 3 and 4). However, the undulations could be controlled through the number of Fourier components during the inverse transform. Lower order Fourier components were robust with respect to

noise. However, they may miss important variation in the data. In this research, the first four Fourier components reproduced the annual trend of natural vegetation reliably and six components reproduced agricultural growing seasons in addition.

5.2. Analysing the effect of Gaussian noise

To simulate data with added Gaussian noise, the pure representative annual profile for each vegetation type was extracted as described in Section 4.2. During this process it was observed that the MTCI values (intra-annual minima to maxima), for the majority of pixels, varied between 2.5 and 3.5 for evergreen, between 2 and 3.5 for semi-evergreen, between 1.25 and 3.5 for moist deciduous and between 1.25 and 3.0 for dry deciduous vegetation types. It was estimated that the mean fluctuation in MTCI value over three years at any single temporal point ranged between 0.1 and 0.25, which amounts to less than 10% of the amplitude difference between the annual MTCI maximum and minimum.

Table 2 provides the performance count of each model under each evaluation criterion (i.e., RMSE, AIC and BIC) for each vegetation type. The number in the table indicates the number of times a model outperformed (i.e., closer fit to the original mean annual profile) the others. It was observed that, in terms of the RMSE, the Fourier approach was more accurate for two vegetation types (evergreen and moist deciduous) and the AG and DL models were more accurate for only one vegetation type. The Whittaker filter resulted as the second best for evergreen and moist deciduous in terms of RMSE. For the AIC and BIC, the DL model outperformed all other approaches. The Fourier approach was the second best for the evergreen vegetation type under both AIC and BIC. Under AIC, AG was most accurate for semi-evergreen but it was the second best in terms of BIC for the same vegetation type. By vegetation type, the AG model had the largest count for semi-evergreen, the Fourier and DL approaches had the largest count for evergreen and moist deciduous, while the DL model performed extremely well for dry deciduous. The Whittaker filter was penalised severely under AIC and BIC.

Table 2

Model performance count using RMSE, AIC and BIC based on a time-series with 1000 realisations of Gaussian noise added (in bold, best fitting models).

Vegetation type	RMSE				AIC				BIC			
	AG	DL	FT	WH	AG	DL	FT	WH	AG	DL	FT	WH
Evergreen	239	170	302	289	165	393	367	75	109	557	327	7
Semi-evergreen	460	121	212	207	386	328	211	75	279	507	200	14
Moist deciduous	79	219	460	242	154	669	140	37	93	806	94	7
Dry deciduous	212	436	150	202	79	487	353	81	47	649	288	16

5.3. Spatial evaluation of fitting techniques

Fig. 6 presents the RMSE calculated, for each pixel, using the four fitted models with parameters tuned to fit a single season growth profile with greater accuracy. Because of this, the resultant RMSE values were larger in the agricultural zones where more than one

annual growing season is common. Interestingly, Fig. 6a and b reveals the major agricultural regions of India depicted in yellow, orange and red colours.

The model parameters were tuned to represent multiple (i.e., two or three) annual growing season patterns and the resulting RMSE is presented in Fig. 7 which shows an evident reduction in RMSE,

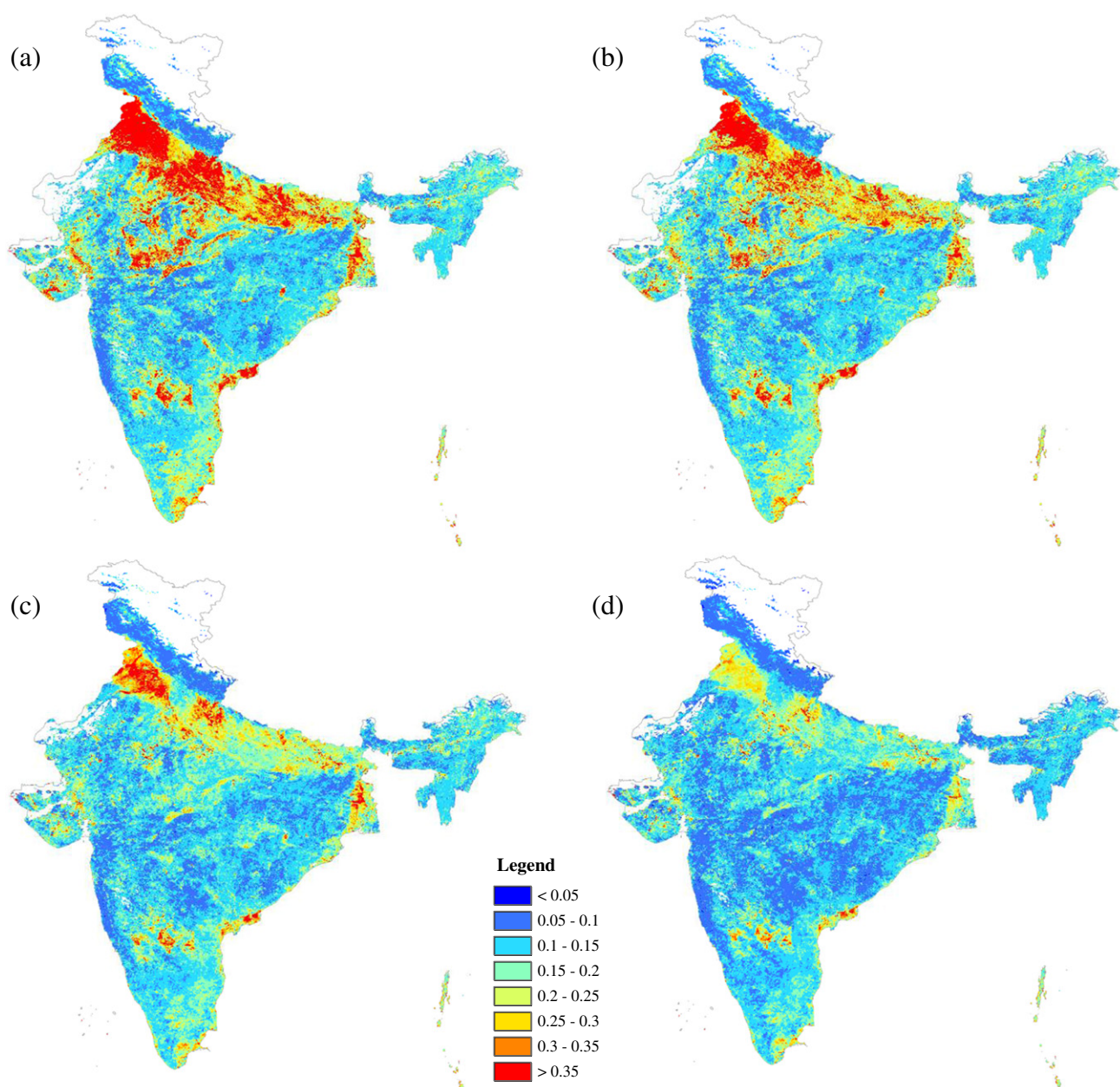


Fig. 6. Root mean square error (RMSE) (year 2004) from four models tuned to fit a single annual growth pattern: (a) double logistic, (b) asymmetric Gaussian, (c) Fourier and (d) Whittaker.

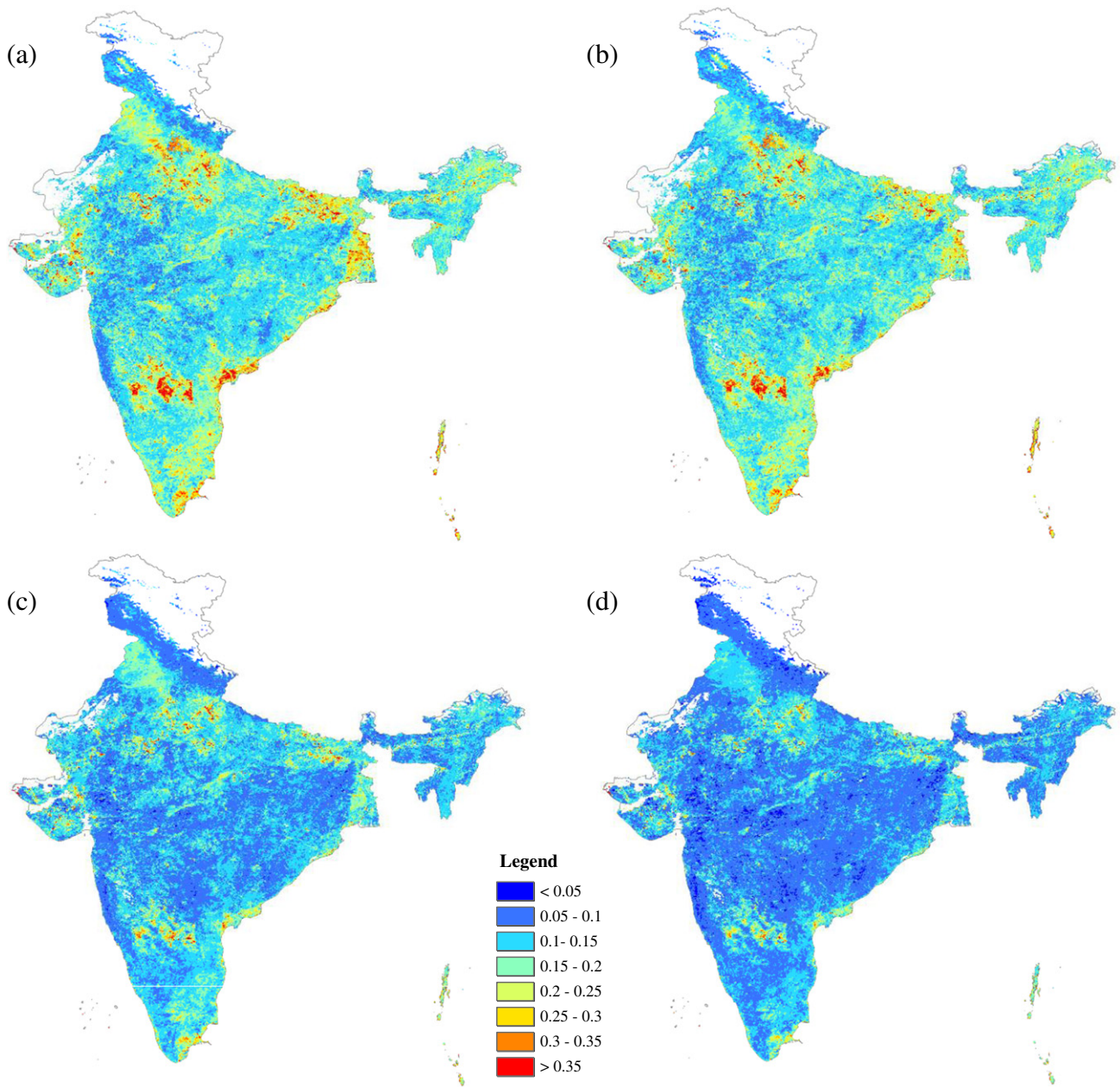


Fig. 7. Root mean square error (RMSE) (year 2004) from four smoothing functions tuned to fit a double annual growth pattern: (a) double logistic, (b) asymmetric Gaussian, (c) Fourier and (d) Whittaker.

particularly over agricultural regions. All four models provided small RMSE values (bluish colour) over natural vegetated regions. However, only the Fourier and Whittaker approaches produced consistently smaller RMSE values over the agricultural as well as natural vegetated regions (Figs. 6c, d and 7c, d).

The RMSEs of each fitted model falling within the homogeneous pixels were extracted and the mean RMSE was calculated within each vegetation type. Table 3 (four harmonics for Fourier; $\lambda = 15$ for Whittaker) presents the mean RMSE from each of the fitted models tuned for a single annual growth pattern. The mean RMSE for two or more annual growth patterns is presented in Table 4 (six harmonics for Fourier; $\lambda = 2$ for Whittaker). The Fourier and Whittaker approaches yielded consistently smaller RMSEs than the other two models. However, the RMSE is not a sufficient indicator of model fit as discussed in Section 4.1 and, hence, the techniques were further evaluated using a residual measure and through the estimated phenological parameters (i.e., OG).

5.3.1. Residuals for pixels with 80% vegetation cover

The mean residual values at 95% confidence interval were calculated for each model tuned for a single season (Fig. 8a,c,e) and for two or more seasons (Fig. 8b,d,f) for the year 2004. These figures reveal the bias and reliability of the fitting models evaluated at each time composite.

5.3.2. Assessing the estimation of phenological parameters

From the fitted models, the OG was calculated for each year. Fig. 9 presents the spatial variation in OG over natural vegetation. The non-forested region was masked in grey colour to provide more effective visualisation of the spatial variation. Agricultural areas were also masked out because of the inherent difficulty in their representation using the selected models: these areas will be scrutinised, in detail, in future research.

It can be seen in Fig. 9 (a to l) that all the models resulted in different spatial distributions in different years, which may be due to annually varying weather conditions. While the arrival of OG seems generally

Table 3
Mean RMSE for different models fitted to time-series for the dominant vegetation types across India (the models are tuned for a single annual growth pattern). (The numbers in the parentheses indicate the number of pure pixels considered in each vegetation type.)

Vegetation type	2004				2005				2006			
	DL	AG	FT	WH	DL	AG	FT	WH	DL	AG	FT	WH
Evergreen (59)	0.151	0.153	0.136	0.126	0.155	0.156	0.142	0.134	0.148	0.150	0.135	0.175
Semi-evergreen (356)	0.148	0.150	0.142	0.126	0.163	0.166	0.151	0.140	0.148	0.150	0.135	0.181
Moist deciduous (387)	0.122	0.130	0.119	0.105	0.119	0.120	0.119	0.106	0.113	0.118	0.108	0.177
Dry deciduous (615)	0.134	0.133	0.121	0.107	0.130	0.126	0.120	0.108	0.127	0.125	0.112	0.187

to vary between years and techniques, the Western Ghats region which runs parallel to the south west coast has a very consistent pattern in all the years and for all techniques. In the central part of India, the OG seems to be later in 2005 which is revealed through orange to red colours. Table 5 provides a summary of the estimated OG values using the different models in the three different years. From all four models, at the national level, it was found that the OG estimates for evergreen vegetation range between DOY 89 and 112, for semi-evergreen vegetation they range between DOY 81 and 120, for moist deciduous they range between DOY 89 and 128 and for dry deciduous they range between DOY 65 and 96. However, the results in Table 5 do not represent regional variability in OG within the same vegetation type, which is dealt with explicitly in Jeganathan et al. (2010a) using Fourier analysis.

The MAD within each of the $1^\circ \times 1^\circ$ grid cells was calculated, for all the years (Fig. 10). It can be seen that the OG values from all four models were similar over natural vegetated regions, as revealed by the lower mean deviation with small variance (bluish colour) (Fig. 10). The deviation was maximum in agricultural regions due to the larger number of annual seasons, as discussed in previous sections.

To provide reliable estimates of the MAD, homogeneous pixels from each vegetation type only were used to calculate the mean and variance of the MAD (Table 6). It was revealed that the deviation was greatest for dry deciduous vegetation. Dry deciduous vegetation is very sensitive to micro-climatic conditions due to poor soil moisture availability. Dry deciduous forest mainly occurs over central India which is also the region where drought is a regular phenomenon. Overall, the models were reliable with an error of one week in most cases as estimated at the whole India level within homogeneous pure vegetation pixels (Table 6).

6. Discussion

Field-based phenological studies are challenging and labour intensive. In only a few countries phenological records are provided within a dense observation network covering more than a few years (e.g., Germany). It is, therefore, important that attention is paid to time-series remotely sensed imagery (delivering continuous observations going back to the 1980s) and, specifically, to the accuracy and reliability of the models used to estimate phenological parameters from these data.

Within the context of mapping phenology from space, many studies have compared different model fitting techniques, mainly using NDVI data, with an emphasis on fitting to the upper envelope and using simple distance measure criteria. The current research used more accurate and robust MERIS MTCI time-series data, where noise can be assumed to be white, and analysed four models in terms of their ability to represent the variation in the annual growth profile and phenology of tropical vegetation types in India over three years (2004 to 2006) using more advanced performance measures.

The present research presented a large array of sample cases from different vegetation types and from different years across the diverse landscape of India. The annual growth rhythm of vegetation types is not constant across years because of varying micro-climatic conditions. The growth rhythm of moist deciduous vegetation type was provided as an example case such as to reveal visually the inter-annual variation and associated fitting results from different techniques in different years. The same was revealed quantitatively in Table 1. The techniques were evaluated using the RMSE, AIC, BIC and a simulated set of noisy time-series data. Fourier analysis has been criticised for its oscillatory nature and difficulties of interpretation in relation to physical ecological phenomena (de Beurs & Henebry, 2010). However, the tests conducted here revealed its advantages in many cases.

All four models were also evaluated using homogeneous pixels of evergreen, semi-evergreen, moist deciduous and dry deciduous vegetation types. It was found that a mean absolute deviation of onset of greenness of three weeks or above was observed within the dry deciduous vegetation type and it was within one to two weeks in evergreen vegetation. All models yielded consistent results over the south-western and north-eastern regions where the forest is dense and protected.

Various views have been expressed in relation to the superiority of different fitting techniques for phenology applications. For example, Beck et al. (2006) found that the DL model was more accurate than the Fourier and Gaussian approaches. Hird and McDermid (2009) found the AG and DL functions to be superior to the Savitzky–Golay, mean-value iteration (MVI), ARMD3-ARMA5 and 4253H techniques. Julien and Sobrino (2009) found that the iterative interpolation for data reconstruction (IDR) technique performed more accurately than the harmonic analysis of NDVI time series (HANTS) algorithm and the DL method. However, their study used a simple distance measure to assess accuracy, which may not be appropriate as it does not consider the number of model parameters used in fitting. Recently,

Table 4
Mean RMSE for different models fitted to time-series for the dominant vegetation types across India (the models are tuned for a double annual growth pattern) (in bold, best fitting models).

Vegetation type	2004				2005				2006			
	DL	AG	FT	WH	DL	AG	FT	WH	DL	AG	FT	WH
Evergreen	0.169	0.171	0.121	0.106	0.171	0.172	0.131	0.116	0.167	0.168	0.127	0.113
Semi-evergreen	0.167	0.169	0.126	0.106	0.182	0.184	0.137	0.119	0.167	0.169	0.122	0.108
Moist deciduous	0.138	0.146	0.103	0.085	0.134	0.136	0.099	0.085	0.127	0.133	0.095	0.082
Dry deciduous	0.135	0.137	0.100	0.084	0.136	0.133	0.102	0.085	0.128	0.127	0.096	0.080

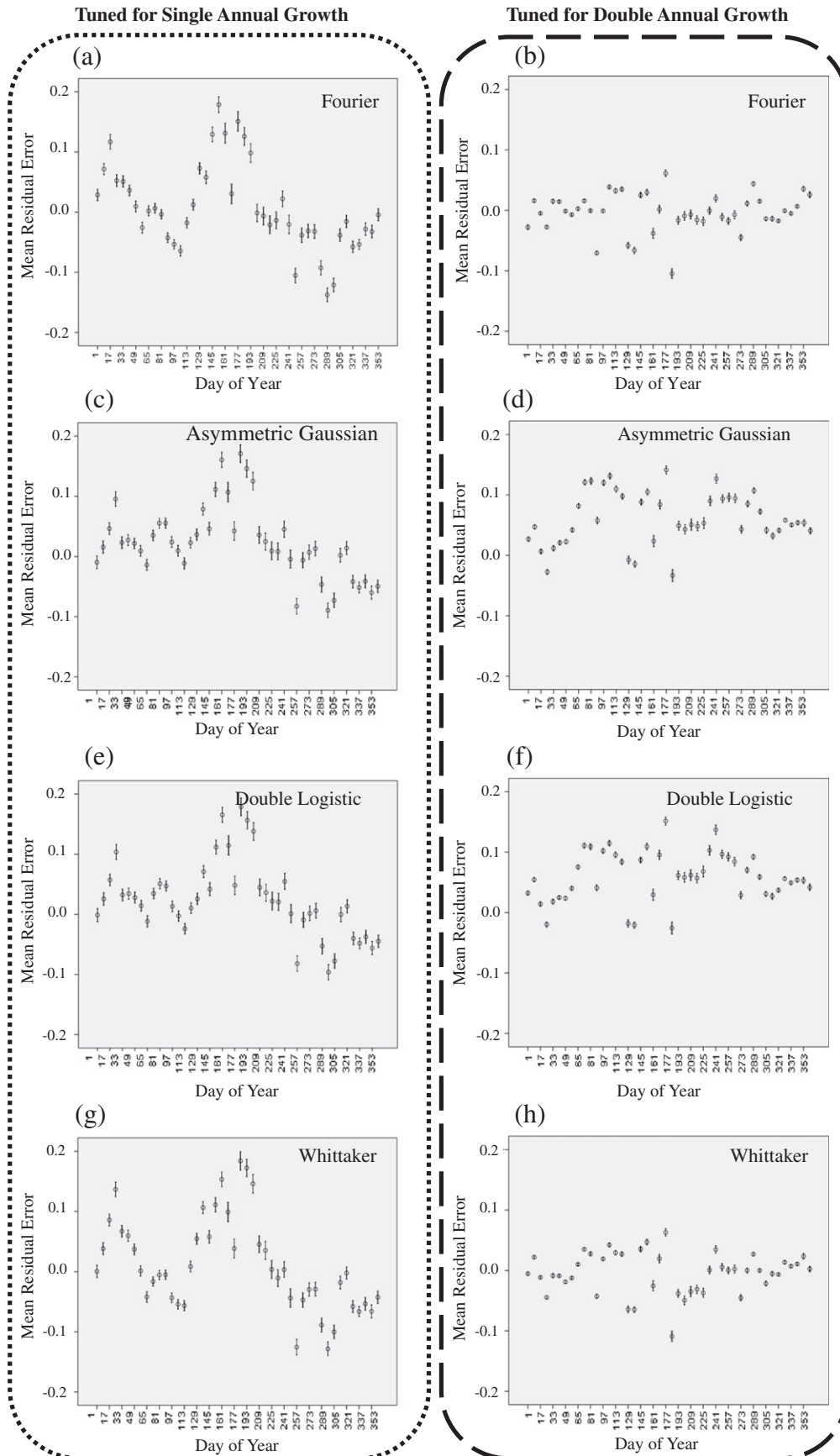


Fig. 8. Mean residual error, with 95% confidence interval, at each date from four models tuned to fit (a, c, e, g) single and (b, d, f, h) double annual growth patterns: (a, b) Fourier, (c, d) asymmetric Gaussian, (e, f) double logistic and (g, h) Whittaker for the year 2004.

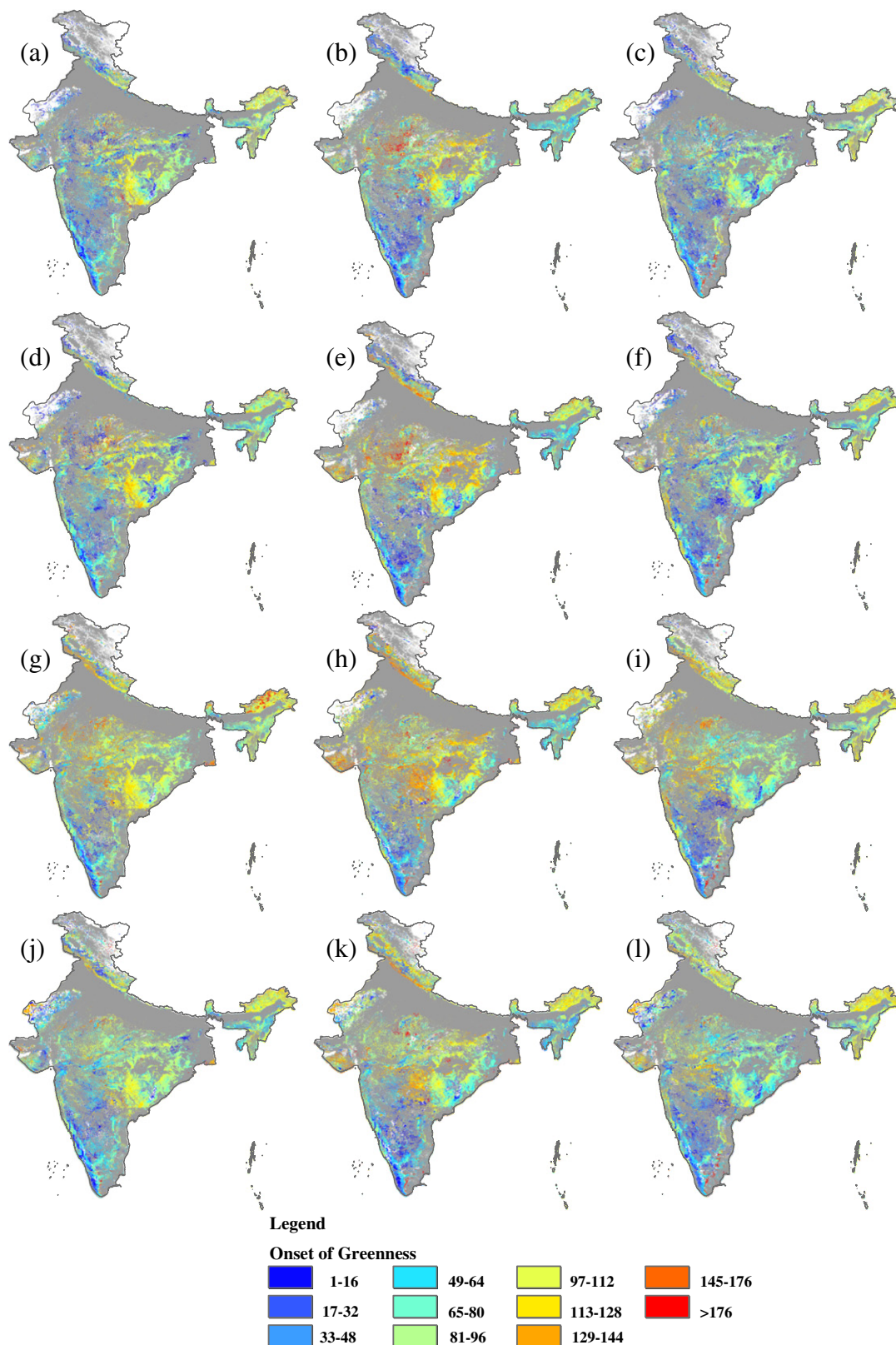


Fig. 9. Estimated onset of greenness (in DOY) for the years (a, d, g, j) 2004, (b, e, h, k) 2005 and (c, f, i, l) 2006 using smoothed data from four models tuned for a single growing season: (a, b, c) asymmetric Gaussian; (d, e, f) double logistic; (g, h, i) Fourier; (j, k, l) Whittaker. Non-forested regions were masked in grey.

de Beurs and Henebry (2010) and White et al. (2009) compared various start-of-spring/season (SOS; OG in the present case) methods, but they could not arrive at a single superior method and revealed that the OG estimates varied amongst the methods. Their work was

done in the USA in temperature-limited vegetation systems with a single annual season, and using Global Inventory Modeling and Mapping Studies (GIMMS) NDVI data. In the present research, MTCI data were used with a focus on diverse and complex landscapes in India

Table 5

Onset of greenness (in DOY), estimated using different techniques, within homogeneous pixels from four major vegetation types in India using majority statistics.

Vegetation type	Year	Fourier	DL	AG	Whittaker
Evergreen	2004	97	105	105	105
	2005	89	89	89	97
	2006	105	105	97	105
Semi evergreen	2004	105	81	97	105
	2005	113	89	97	105
	2006	105	105	97	105
Moist deciduous	2004	105	97	89	97
	2005	121	121	105	97
	2006	89	89	89	97
Dry deciduous	2004	89	73	81	73
	2005	73	97	65	89
	2006	73	73	81	81

where rainfall is the major driving factor for greening and, hence, noisier observations and greater inter-annual variability in OG result (de Beurs & Henebry, 2010).

The Whittaker smoother has not been evaluated in the past in specific relation to phenology, and in the current study it performed well in terms of the RMSE (Table 1). The main issue with the Whittaker filter is the choice of an optimal model parameter to avoid over fitting. While it performed well in terms of the RMSE, the Whittaker filter with $\lambda = 2$ did not perform well in terms of the AIC and BIC criteria because of its large number of effective model parameters. However, Whittaker fitting with $\lambda = 15$ outperformed other approaches for the raw data, but did not perform well under the simulated noise scenario. Based on RMSE, AIC and BIC derived with respect to the sample data (Figs. 3 to 5 and Tables 1 and 2), the Whittaker and Fourier approaches were preferable to the DL and AG models, but the DL and AG models did produce

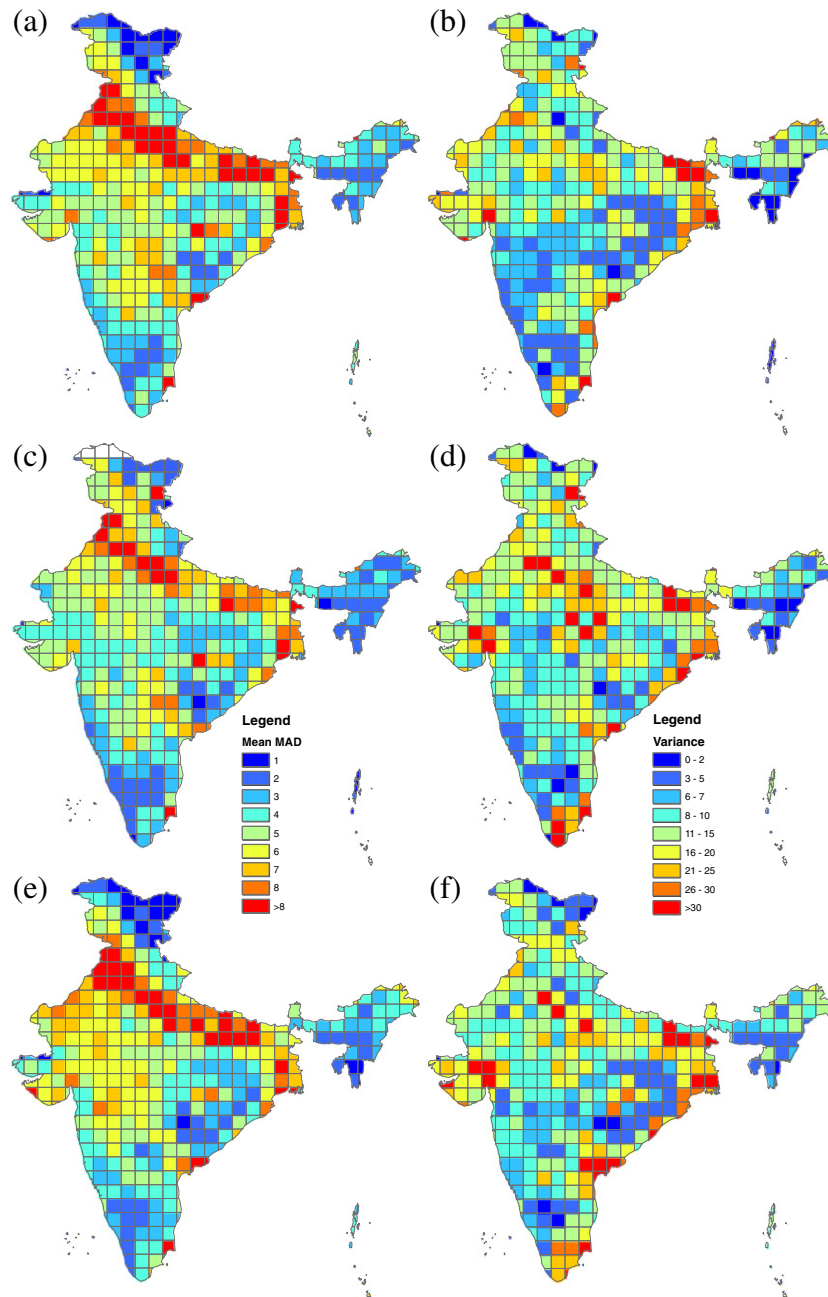


Fig. 10. (a,c,e) Mean and (b,d,f) variance of mean absolute difference (MAD) in estimated onset of greenness (in composite numbers, ~8 days), using smoothed data from four models tuned for a single growing season, within $1^\circ \times 1^\circ$ national grid cells for the years (a, b) 2004, (c, d) 2005 and (e, f) 2006.

Table 6

Statistics (mean and variance of MAD) for the onset of greenness estimated for homogeneous pixels of four major vegetation types in India.

Vegetation type	Year	Mean (in weeks)	Variance (in weeks)
Evergreen	2004	1.09	1.02
	2005	1.13	1.49
	2006	1.09	1.90
Semi-evergreen	2004	1.81	4.16
	2005	1.87	4.16
	2006	1.56	4.12
Moist deciduous	2004	1.35	1.96
	2005	2.14	3.24
	2006	1.57	3.84
Dry deciduous	2004	3.14	7.08
	2005	3.76	8.70
	2006	3.15	7.24

a low AIC and BIC for a few samples. When a large number of data were simulated with Gaussian noise, the DL model outperformed the others. This implies that DL is less affected by Gaussian noise, in most of the cases, and it fitted well for a single growing season vegetative species such as moist deciduous in our case. Further analysis revealed that the error variance between the Fourier and DL approaches was not significantly different, and hence, the major reason for the better performance of the DL model was due to the difference in the number of free parameters (k) (for Fourier, $k=7$; for DL, $k=6$) in the AIC and BIC calculations. When the models were checked in terms of phenological estimation of OG (Table 5, Table 6), all the models yielded close results with a mean difference of 1 week (i.e., 1 temporal composite), which is encouraging from the user's point of view. However, in the present study it was found that the DL and AG approaches were not accurate in representing annual growth pattern data where there were two or more seasons, especially over agricultural regions.

It was observed that the residual error in 2004 was larger relative to other years for all models. To understand the reason, the residual error was analysed within each class and it was found that the larger deviation was due mainly to moist deciduous and dry deciduous pixels. Interestingly, the cause for this deviation was attributed to fluctuations in the MTCI values, attributable to non-uniform rainfall during the growing season as rainfall and vegetation cover are strongly interlinked in India (Prasad et al., 2007). To investigate this link, historical data on drought were consulted and it was found that there was a recurring drought for the three consecutive years (2001–02, 2002–03, 2003–04) in Karnataka, Maharashtra, Jharkhand and many other central Indian states (Biradar & Sridhar, 2009; PACS, 2009) where the moist and dry deciduous vegetation types mainly occur. Hence, untimely rainfall could potentially affect the growth pattern of these two vegetation types along with its potential impact on agricultural crops. The residual error from the AG and DL models was positively biased (Fig. 8) whereas the Fourier and Whittaker approaches were less biased.

Vegetation growth patterns depend on a multitude of factors. However, in the tropics the main influencing factors are rainfall and temperature. The onset of greenness in India is linked mainly to rainfall, but in northern latitudinal countries it is mostly temperature driven. Climate change projections have forecasted increases in Indian monsoon precipitation and extreme temperatures (Rupa Kumar et al., 2006) and the impact of such changes on vegetation phenology is still an intriguing research area. Although Dash et al. (2010) and Jeganathan et al. (2010a, 2010b) studied phenological parameters in India, they did not reveal the uncertainty associated with their approach, and also did not study long-term changes in phenology of Indian vegetation. Hence, it would be interesting to monitor changes in phenology over the last few decades and into the future in India. For such research, the current study provides valuable information about the intricacies of model choice and fitting, and associated errors in phenology extraction.

7. Conclusion

Continuous spatial information about vegetation growth and phenology is a potentially pivotal input to modelling primary productivity, biomass and natural carbon dynamics. The research presented here provides an important comparative analysis of the capability of four different models for smoothing remotely sensed time-series and estimating phenological parameters over the tropical landscapes of India. For data extracted from remotely sensed images, the Whittaker approach outperformed the others, but its underperformance when applied to noisy data raises some concerns. When simulated noise was added, the DL model outperformed the others, but performed less well on the real data. The Fourier approach performed consistently well in representing both the image data and the synthetic (noisy) data. No single model exhibited a consistently superior performance under all tests. Hence, caution is needed with regard to the applicability of each approach for specific study areas and, moreover, care is needed to determine: the number of harmonics for Fourier, λ for Whittaker, and parameters such as the number of seasons and the outlier threshold for the DL and AG models.

The inter-comparisons presented in this paper provide an important source of information on the quality of fitted phenological curves and estimated parameters. This information on uncertainty, and the effects of model choice on phenological parameter estimates, should be of value in a range of studies that attempt to characterise vegetation phenology from space. The variation in estimates observed between the approaches sets the scene for the possibility of combining different estimates of phenological parameters (e.g., from different sensors, different models and different research groups), through a statistical ensemble-based approach. Overall, the study fulfilled the objective of checking the models' ability to reproduce discernible phenological patterns adequately and their robustness to random temporal fluctuations. The information provided here on the uncertainty in estimates of phenology across India may also be important in relation to efforts to establish a phenological network in India (Moza and Bhatnagar 2005, Kushwaha and Singh 2008).

References

- Akaike, H. (1973). Information theory & an extension of the maximum likelihood principle. In B. N. Petrov, & F. Csaki (Eds.), *2nd International Symposium on Information Theory* (pp. 267–281). Budapest: Akademiai Kiado.
- Atkinson, P. M., Jeganathan, C., & Dash, J. (2009). Analysing the effect of different geocomputational techniques on estimating phenology in India. In B. G. Lees, & S.W. Laffan (Eds.), *10th International Conference on GeoComputation*. Sydney: UNSW November–December, 2009.
- Atzberger, C., & Eilers, P. H. C. (2011a). A time series for monitoring vegetation activity and phenology at 10-daily time steps covering large parts of South America. *International Journal of Digital Earth*, 4(5), 365–386.
- Atzberger, C., & Eilers, P. H. C. (2011b). Evaluating the effectiveness of smoothing algorithms in the absence of ground reference measurements. *International Journal of Remote Sensing*, 32(13), 3689–3709.
- Bartholome, E., & Belward, A. S. (2005). GLC2000: A new approach to global land cover mapping from Earth observation data. *International Journal of Remote Sensing*, 26(5), 1959–1977.
- Beck, P. S. A., Atzberger, C., Hogda, K. A., Johansen, B., & Skidmore, A. K. (2006). Improved monitoring of vegetation dynamics at very high latitudes: A new method using MODIS NDVI. *Remote Sensing of Environment*, 100, 321–334.
- Biradar, N., & Sridhar, K. (2009). Consequences of 2003 drought in Karnataka with particular reference to livestock & fodder. *Journal of Human Ecology*, 26(2), 123–130.
- Bradley, Bethany A., Jacob, Robert W., Hermance, John F., & Mustard, John F. (2007). A curve fitting procedure to derive inter-annual phenologies from time series of noisy satellite NDVI data. *Remote Sensing of Environment*, 106(2), 137–145.
- Chen, J., Jönsson, P., Tamura, M., Gu, Z., Matsuhashita, B., & Eklundh, L. (2004). A simple method for reconstructing a high-quality NDVI time-series data set based on the Savitzky–Golay filter. *Remote Sensing of Environment*, 91, 332–344.
- Cleland, E. E., Chuine, I., Menzel, A., Mooney, H. A., & Schwartz, M. D. (2007). Shifting plant phenology in response to global change. *Trends in Ecology & Evolution*, 22(7), 357–365.
- Curran, P. J., & Steele, C. M. (2005). MERIS: The re-branding of an ocean sensor. *International Journal of Remote Sensing*, 26, 1781–1798.
- Dash, J., & Curran, P. J. (2004). The MERIS terrestrial chlorophyll index. *International Journal of Remote Sensing*, 25, 5403–5413.

- Dash, J., & Curran, P. J. (2007). Evaluation of the MERIS Terrestrial Chlorophyll Index (MTCI). *Advances in Space Research*, 39(1), 100–104.
- Dash, J., Jeganathan, C., & Atkinson, P. M. (2010). The use of MERIS Terrestrial Chlorophyll Index to study spatio-temporal variation in vegetation phenology over India. *Remote Sensing of Environment*, 114, 1388–1402.
- Dash, J., Lankester, T., Hubbard, S., & Curran, P. J. (2008). Signal to noise ratio for MTCI & NDVI time series data. *Proceedings of the 2nd MERIS/(A)ATSR User Workshop, Frascati, Italy, 22–26 September 2008*.
- De Beurs, K. M., & Henebry, G. M. (2010). Spatio-temporal statistical methods for modelling land surface phenology. In I. L. Hudson, & M. R. Keatley (Eds.), *Phenological research*. Springer Science + Business Media, B.V. http://dx.doi.org/10.1007/978-90-481-3335-2_9.
- Eilers, P. H. C. (2003). A perfect smoother. *Analytical Chemistry*, 75(14), 3631–3636.
- Eilers, P. H. C., & Marx, B. D. (1996). Flexible smoothing with B-splines and penalties. *Statistical Science*, 11(2), 89–121.
- Geerken, R. A. (2009). An algorithm to classify & monitor seasonal variations in vegetation phenologies & their inter-annual change. *ISPRS Journal of Photogrammetry and Remote Sensing*, 64, 422–431.
- Gitelson, A., & Kaufman, Y. (1998). MODIS NDVI optimization to fit the AVHRR data series—Spectral considerations. *Remote Sensing of Environment*, 66(3), 343–350.
- Hermance, J. F., Jacob, R. W., Bradley, B. A., & Mustard, J. F. (2007). Extracting phenological signals from multiyear AVHRR NDVI time series: Framework for applying high-order annual splines with roughness damping. *IEEE Transactions on Geoscience and Remote Sensing*, 45(10), 3264–3276 October.
- Hird, J. N., & McDermid, G. J. (2009). Noise reduction of NDVI time series: An empirical comparison of selected techniques. *Remote Sensing of Environment*, 113(1), 248–258.
- Holben, B. N. (1986). Characteristics of maximum-values composite images from temporal AVHRR data. *International Journal of Remote Sensing*, 7, 1417–1434.
- Huete, A., Didan, K., Miura, T., Rodríguez, E. P., Gao, X., & Ferreira, L. G. (2002). Overview of the radiometric and biophysical performance of the MODIS vegetation indices. *Remote Sensing of Environment*, 83, 195–213.
- Jakubauskas, M. E., Legates, D. R., & Kastens, J. H. (2001). Harmonic analysis of time-series AVHRR NDVI data. *Photogrammetric Engineering and Remote Sensing*, 67, 461–470.
- Jeganathan, C., Dash, J., & Atkinson, P. M. (2010a). Characterising the spatial pattern of phenology for the tropical vegetation of India using multi-temporal MERIS chlorophyll data. *Landscape Ecology*, 25, 1125–1141.
- Jeganathan, C., Dash, J., & Atkinson, P. M. (2010b). Mapping the phenology of natural vegetation in India using a remote sensing-derived chlorophyll index. *International Journal of Remote Sensing*, 31(22), 5777–5796.
- Jeong, S. J., Ho, C. H., Gim, H. J., & Brown, M. E. (2011). Phenology shifts at start vs. end of growing season in temperate vegetation over the Northern Hemisphere for the period 1982–2008. *Global Change Biology*. <http://dx.doi.org/10.1111/j.1365-2486.2011.02397.x>.
- Jönsson, P., & Eklundh, L. (2002). Seasonality extraction by function fitting to time-series of satellite sensor data. *IEEE Transactions on Geoscience and Remote Sensing*, 40, 1824–1832.
- Jönsson, P., & Eklundh, L. (2004). TIMESAT—A program for analysing time-series of satellite sensor data. *Computers & Geosciences*, 30, 833–845.
- Jönsson, P., & Eklundh, L. (2006). TIMESAT—a program for analysing time-series of satellite sensor data. *Users Guide for TIMESAT 2.3*. Lund: Lund University Available online at http://www.nateko.lu.se/personal/Lars.Eklundh/TIMESAT/timesat2_3_users_manual.pdf.
- Joshi, P. K., Roy, P. S., Singh, S., Agrawal, S., & Yadav, D. (2006). Vegetation cover mapping in India using multi-temporal IRS wide Field Sensor WiFS data. *Remote Sensing of Environment*, 103, 190–202.
- Julien, Y., & Sobrino, J. A. (2009). Global land surface phenology trends from GIMMS database. *International Journal of Remote Sensing*, 30(13), 3495–3513.
- Kushwaha, C. P., & Singh, K. P. (2008). India needs phenological stations network. *Current Science*, 95, 832–834.
- Lu, X., Liu, R., Liu, J., & Liang, S. (2007). Removal of noise by wavelet method to generate high quality temporal data of terrestrial MODIS products. *Photogrammetric Engineering and Remote Sensing*, 73(10), 1129–1139.
- Malingreau, J. P. (1986). Global vegetation dynamics: Satellite observations over Asia. *International Journal of Remote Sensing*, 7, 1121–1146.
- Menzel, A. (2002). Phenology: Its importance to global change community, an editorial comment. *Climate Change*, 54, 379–385.
- Moody, A., & Johnson, D. (2001). Land-surface phenologies from AVHRR using the discrete Fourier transform. *Remote Sensing of Environment*, 75, 305–323.
- Moza, M. K., & Bhatnagar, A. K. (2005). Phenology and climate change. *Current Science*, 89, 243–244.
- Mutanga, O., & Skidmore, A. K. (2004). Narrow band vegetation indices overcome the saturation problem in biomass estimation. *International Journal of Remote Sensing*, 25(19), 3999–4014.
- Myneni, R. B., Keeling, C. D., Tucker, C. J., Asrar, G., & Nemani, R. R. (1997). Increased plant growth in the northern high latitudes from 1981 to 1991. *Nature*, 386, 698–702.
- PACS (2009). Drought in India: Challenges and initiatives. *Poorest Areas Civil Society (PACS) Programme 2001–2008. Info Change, Pune, India* Available online at: <http://www.empowerpoor.org/downloads/drought1.pdf>.
- Parmesan, C. (2007). Influences of species, latitudes and methodologies on estimates of phenological response to global warming. *Global Change Biology*, 13, 1860–1872.
- Parmesan, C., & Yohe, G. (2003). A globally coherent fingerprint of climate change impacts across natural systems. *Nature*, 421, 37–42.
- Pinzon, J. (2002). Using HHT to successfully uncouple seasonal and interannual components in remotely sensed data. *Proceedings of the 6th World Multiconference on Systematics, Cybernetics and Informatics (SCI 2002), Orlando, USA, XIV*. (pp. 287–292).
- Pinzon, J., Brown, M. E., & Tucker, C. J. (2004). Satellite time series correction of orbital drift artefacts using empirical mode decomposition. In N. E. Huang, & S. S. P. Shen (Eds.), *EMD & Its Applications*, 10. (pp. 285–295) Singapore: World Scientific.
- Prasad, A. K., Sarkar, S., Singh, R. P., & Kafatos, M. (2007). Inter-annual variability of vegetation cover and rainfall over India. *Advances in Space Research*, 39, 79–87.
- Reed, B. C., Brown, J. F., VanderZee, D., Loveland, T. R., Merchant, J. W., & Ohlen, D. O. (1994). Measuring phenological variability from satellite imagery. *Journal of Vegetation Science*, 5, 703–714.
- Roerink, G. J., Menenti, M., & Verhoef, W. (2000). Reconstructing cloud free NDVI composites using Fourier analysis of time series. *International Journal of Remote Sensing*, 21(9), 1911–1917.
- Root, T. L., Price, J. T., Hall, K. R., Schneider, S. H., Rosenzweig, C., & Pounds, J. A. (2003). Finger prints of global warming on wild animals and plants. *Nature*, 421, 57–60.
- Rupa Kumar, K., Sahai, A. K., Krishna Kumar, K., Patwardhan, S. K., Mishra, P. K., Revadehar, J. V., et al. (2006). High-resolution climate change scenarios for India for the 21st Century. *Current Science*, 90(3), 334–345.
- Sakamoto, T., Yokozawa, M., Toritani, H., Shibayama, M., Ishitsuka, N., & Ohno, H. (2005). A crop phenology detection method using time-series MODIS data. *Remote Sensing of Environment*, 96, 366–374.
- Schwarz, G. (1978). Estimating the dimension of a model. *The Annals of Statistics*, 6, 461–464.
- SFR (2009). *State of Forest Report 2009*. Dehradun, India: Forest Survey of India Available online at: http://www.fsi.nic.in/sfr_2009.htm.
- Stibig, H. J., Belward, A., Roy, P. S., Rosalina-Wasrin, Agrawal, S., Joshi, P. K., et al. (2007). A land-cover map for South and Southeast Asia derived from SPOT-VEGETATION data. *Journal of Biogeography*, 34, 625–637.
- Tucker, C. J., Pinzon, J. E., Brown, M. E., Slayback, D., Pak, E. W., Mahoney, R., et al. (2005). An extended AVHRR 8-km NDVI data set compatible with MODIS & SPOT vegetation NDVI data. *International Journal of Remote Sensing*, 26(20), 4485–4498.
- Verhoef, W., Menenti, M., & Azzali, S. (1996). A colour composite of NOAA-AVHRRNDVI based on time series (1981–1992). *International Journal of Remote Sensing*, 17, 231–235.
- Vilela, M., Borges, C. C. H., Vinga, S., Vasconcelos, A. T. R., Santos, H., Voit, E. O., et al. (2007). Automated smoother for the numerical decoupling of dynamics models. *BMC Bioinformatics*. <http://dx.doi.org/10.1186/1471-2105-8-305>.
- Wagenseil, H., & Samimi, C. (2006). Assessing spatio-temporal variations in plant phenology using Fourier analysis on NDVI time series: Results from a dry savannah environment in Namibia. *International Journal of Remote Sensing*, 27, 3455–3471.
- White, M. A., De Beurs, K. M., Didan, K., Inouye, D. W., Richardson, A. D., Jensen, O. P., et al. (2009). Intercomparison, interpretation, & assessment of spring phenology in North America estimated from remote sensing for 1982–2006. *Global Change Biology*, 15, 2335–2359.
- White, M. A., Hoffman, F., Hargrove, W. W., & Nemani, R. R. (2005). A global framework for monitoring phenological responses to climate change. *Geophysical Research*, 32, L04705. <http://dx.doi.org/10.1029/2004GL021961>.
- Yu, X., Zhuang, D., Hou, X., & Chen, H. (2005). Forest phenological patterns of Northeast China inferred from MODIS data. *Journal of Geographical Sciences*, 15(2), 239–246.
- Zhang, X. Y., Friedl, M. A., Schaaf, C. B., Strahler, A. H., Hodges, J. C. F., Gao, F., et al. (2003). Monitoring vegetation phenology using MODIS. *Remote Sensing of Environment*, 84, 471–475.